Control of leaf expansion: a developmental switch from metabolics to hydraulics

Florent Pantin, Thierry T. Simonneau, Gaelle Rolland, Myriam Dauzat, Bertrand Muller

Control of Leaf Expansion: A Developmental Switch from Metabolics to Hydraulics[1][W][OA]

Florent Pantin, Thierry Simonneau, Gaëlle Rolland, Myriam Dauzat, and Bertrand Muller*

Laboratoire d'Ecophysiologie des Plantes sous Stress Environnementaux, UMR759, Institut de Biologie Intégrative des Plantes, INRA, 34060 Montpellier, France

Leaf expansion is the central process by which plants colonize space, allowing energy capture and carbon acquisition. Water and carbon emerge as main limiting factors of leaf expansion, but the literature remains controversial about their respective contributions. Here, we tested the hypothesis that the importance of hydraulics and metabolics is organized according to both dark/light fluctuations and leaf ontogeny. For this purpose, we established the developmental pattern of individual leaf expansion during days and nights in the model plant Arabidopsis (*Arabidopsis thaliana*). Under control conditions, decreases in leaf expansion were observed at night immediately after emergence, when starch reserves were lowest. These nocturnal decreases were strongly exaggerated in a set of starch mutants, consistent with an early carbon limitation. However, low-light treatment of wild-type plants had no influence on these early decreases, implying that expansion can be uncoupled from changes in carbon availability. From 4 d after leaf emergence onward, decreases of leaf expansion were observed in the daytime. Using mutants impaired in stomatal control of transpiration as well as plants grown under soil water deficit or high air humidity, we gathered evidence that these diurnal decreases were the signature of a hydraulic limitation that gradually set up as the leaf developed. Changes in leaf turgor were consistent with this pattern. It is concluded that during the course of leaf ontogeny, the predominant control of leaf expansion switches from metabolics to hydraulics. We suggest that the leaf is better armed to buffer variations in the former than in the latter.

Leaf expansion is a major component of plant performance. It enables light capture, which powers photosynthesis and thus biomass production. It is also one of the first plant functions affected by environmental stresses such as water deficit (Hsiao, 1973), making it a key target for identifying tolerant genotypes and species (Tardieu and Tuberosa, 2010). To this aim, understanding the processes dominating the control of leaf expansion is a crucial step. Among the multiplicity of factors involved in leaf expansion, two major limitations emerge: a biophysical control mainly linked to water fluxes to growing cells, and a metabolic control linked to the supply of carbohydrates (Dale, 1988; Walter et al., 2009).

To some extent, plants can be represented as systems ruled by biophysical laws, with water fluxes modeled as Ohm-like functions of hydraulic conductances and water potentials (van den Honert, 1948). In line with the formalism of Lockhart (1965), several arguments support the view that leaf expansion is predominantly driven by cell turgor, itself largely induced by soil water potential and transpiration. Notably, increasing soil water deficit (Boyer, 1968; Acevedo et al., 1971) or evaporative demand (Ben-Haj-Salah and Tardieu, 1997; Tardieu et al., 2000) leads to growth inhibitions that correlate in space and time with turgor depressions in the elongating zone of maize (*Zea mays*) leaves (Bouchabké et al., 2006; Ehlert et al., 2009). Such inhibitions under limited water availability have been attributed to a collapse of water potential gradients that govern water fluxes to growing cells (Boyer, 1988; Tang and Boyer, 2002, 2008). Hydraulic control of growth is thus thought to be more restrictive during the day than during the night, a period during which stomatal closure allows the recovery of leaf water potential (Ben-Haj-Salah and Tardieu, 1997).

While cell expansion needs water to proceed, it also requires energy and carbon skeletons and therefore relies on assimilates supplied to the growing tissues (Dale, 1985; Smith and Stitt, 2007). Consistent with this, growth appears to be closely controlled by carbon metabolism at different scales. Most current agronomical models are based on the formalism of Monteith (1977), linking biomass accumulation to radiation intercepted by plants and carbon assimilation rate. Likewise, stable correlations are observed between organ growth rates and intercepted radiation or carbohydrate availability in their growing parts, such as in roots (Aguirrezabal et al., 1994; Freixes et al., 2002) or reproductive organs (Dosio et al., 2011). Finally, the leaf growth rhythm of several species at a fine

[1] This work was supported by the French Ministry of Research (grant to F.P.) and by the European Commission (FP6) through the AGRON-OMICS Integrated Project (grant no. LSHG–CT–2006–037704).

* Corresponding author; e-mail muller@supagro.inra.fr.

The author responsible for distribution of materials integral to the findings presented in this article in accordance with the policy described in the Instructions for Authors (www.plantphysiol.org) is: Bertrand Muller (muller@supagro.inra.fr).

[W] The online version of this article contains Web-only data.

[OA] Open Access articles can be viewed online without a subscription.

www.plantphysiol.org/cgi/doi/10.1104/pp.111.176289

time scale coincides with fluctuations in carbohydrate availability (Walter and Schurr, 2005; Wiese et al., 2007). To accommodate fluctuations in photosynthetically active radiation, carbon availability is buffered by transient storage compounds, especially starch, which is accumulated during the day and used as a carbon supply at night. The rate of nocturnal starch breakdown is under fine control to allow optimum exhaustion of carbon stores by the end of the night without entering carbon starvation, which has deleterious effects on various metabolic and developmental processes (Brouquisse et al., 1991; Smith and Stitt, 2007). This turnover of starch reserves is thought to be a major integrator in the regulation of growth (Sulpice et al., 2009).

To what extent leaf ontogeny may interfere with metabolic and hydraulic factors constraining leaf growth is not known. Still, expectations can yet be drawn from basic knowledge of the sink-to-source transition in developing leaves. Since young leaves critically depend on carbon import from older leaves (Turgeon, 1989), their expansion could be expected to be more dependent upon carbon fluctuations as compared with older leaves, which have a positive carbon balance. On the other hand, young leaves could be prioritized in such a way that the carbon supply to them is maintained when the whole plant carbon availability is decreased (Minchin et al., 1993; Lacointe and Minchin, 2008). In the same way, possible interactions between ontogeny and hydraulics can only be speculated. For instance, water supply through xylem vessels could decrease with leaf maturation as a result of decreased hydraulic conductivity (Martre et al., 2000, 2001; Martre and Durand, 2001; Nardini et al., 2010). On the other hand, it is generally admitted that cuticle thickens with leaf development (Richardson et al., 2007), suggesting that this could limit passive water loss (Kerstiens, 2006) and favor hydraulic status as the leaf expands. Finally, although the molecular events leading to stomatal formation are now well described (Bergmann and Sack, 2007), the acquisition of stomatal functionality during leaf development remains unclear. Thus, quantitative arguments that distinguish the possible roles of water relations or carbon availability on expansion during leaf ontogeny are lacking.

In this study, we aimed to discover the relative contributions of water and carbon to the control of growth with respect to leaf ontogeny in the model plant Arabidopsis (*Arabidopsis thaliana*). For this purpose, we evaluated at a day/night time step the developmental pattern of leaf expansion in mutants impaired in starch synthesis or breakdown as well as in mutants deregulated in stomatal control of transpiration. Furthermore, plants were grown under various levels of soil water content, air humidity, and irradiance. Results converge to associate hydraulic and metabolic controls to day and night periods, respectively. Evidence is then presented that during its development, the leaf experiences first metabolic and then hydraulic limitation. Both genetic and environmental cues act to modulate metabolic or hydraulic constraints and to shift in a consistent way the timing when the main limitation switches from carbon to water.

RESULTS AND DISCUSSION

A Dual Pattern in the Wild-Type Plants

In Arabidopsis, the expansion of one individual leaf from initiation at the shoot apical meristem to growth cessation can last more than 1 month (Aguirrezabal et al., 2006). Because whole plant characteristics (e.g. sink-source balance; Christophe et al., 2008) can change substantially over such a long period, we designed a protocol to study day/night changes of relative expansion rate (RER) at different leaf growth stages over a much shorter time scale. Briefly, we used the expansion of 10 to 13 serial leaves over 24 h to reconstruct the expansion pattern of an individual leaf over 8 to 10 d. This process, driven by the concept of phyllochron age, is described in "Materials and Methods" and fully detailed in Supplemental Materials and Methods S1 and in Supplemental Figures S1 to S3. We focused on a developmental window encompassing the first half of leaf expansion after emergence, a period during which relative and then absolute leaf expansion are successively maximum (Supplemental Fig. S1) and therefore strongly contribute to final leaf area. Under well-watered conditions ($0.35\ g_{water}\ g^{-1}_{dry\ soil}$), a common RER pattern emerged (Fig. 1) in both ecotype Columbia (Col-0) and ecotype Wassilewskija (Ws-3). Two successive periods could be distinguished along the overall decreasing pattern of RER. The first one took place early after emergence for about 3 d and showed leaf expansion rate being on average 0.15 and 0.23 d^{-1} higher during light than during dark phases for Col-0 and Ws-3, respectively. The second period occurred at later stages at 5 d following emergence and showed RER being, by contrast, on average 0.16 and 0.08 d^{-1} higher during the dark phases. For the sake of clarity and to allow statistical analysis, RER patterns were then parameterized by fitting a second-degree polynomial independently to the day and night RER, as shown for Col-0 in the inset of Figure 1. We hypothesized that late alternations (RER night $>$ RER day) reflect hydraulic limitations while early alternations (RER day $>$ RER night) reflect metabolic limitations. To test these hypotheses, we altered the hydraulic and metabolic status of the leaf using genetic and environmental manipulations.

Daytime Reductions in Leaf Expansion Are under Hydraulic Control: Evidence from Stomatal Mutants, Soil Water Deficit, and High Air Humidity

Daytime drops of leaf expansion as observed here in Arabidopsis recall results repeatedly observed in monocots such as maize (Ben-Haj-Salah and Tardieu,

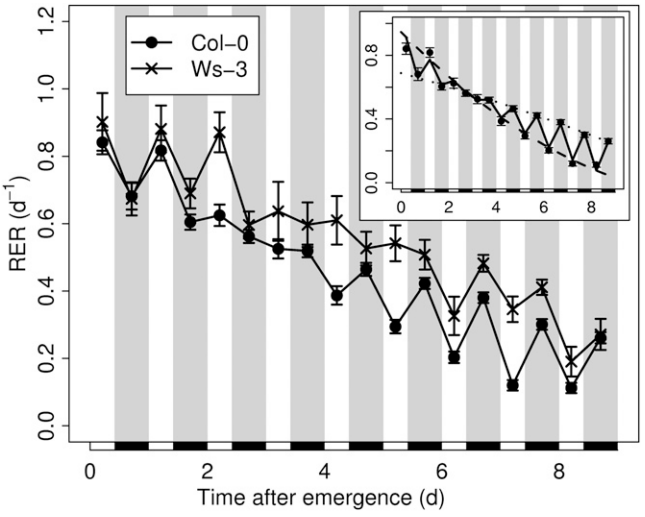

Figure 1. Expansion patterns of the wild-type plants under well-watered conditions. The day and night RERs were monitored on Col-0 (black circles) and Ws-3 (crosses) from leaf emergence to mid development (see "Materials and Methods"; Supplemental Fig. S1). The inset shows the smoothing process for the RER. As shown here for Col-0, a second-degree polynomial was fitted independently to the day RER (dotted line) and to the night RER (solid line). Then, the growth patterns were drawn from leaf emergence to leaf mid development by joining the predicted values for the successive light and dark periods. The same units are used for the main graph and the inset. Black rectangles and gray bands indicate the night periods. Values shown are means ± SE ($n \geq 10$).

1997; Tang and Boyer, 2002; Bouchabké et al., 2006), wheat (*Triticum aestivum*; Christ, 1978), rice (*Oryza sativa*; Cutler et al., 1980), fescue (*Festuca arundinacea*; Schnyder and Nelson, 1988; Durand et al., 1995), or *Miscanthus* (Clifton-Brown and Jones, 1999) and also in dicots such as sunflower (*Helianthus annuus*; Boyer, 1968) or several halophytic species (Rozema et al., 1987). Either permanent or transient, these drops have been attributed to a hydraulic limitation, because they occurred especially under restricted water availability (i.e. under transpiring conditions with higher amplitude under soil water deficit). We thus tested if the decrease of expansion during days could be due to an impairment of leaf water potential induced by transpiration. We analyzed the *abscisic acid deficient4* (*aba4*) mutant (North et al., 2007) and the *9-cis-epoxycarotenoid dioxygenase6* overexpressor (*NCED6-OE*) transformant (Lefebvre et al., 2006) reputed to have high and low stomatal conductance, respectively, due to modified capacities to synthesize abscisic acid (ABA). Stomatal conductance of the *aba4* mutant was significantly higher in our conditions as compared with the wild-type, while photosynthesis rate was not affected by the mutation (Fig. 2A, inset). Hence, we expected the effect of the hydraulic constraint on leaf expansion to be amplified in this mutant. In a consistent way, *aba4* showed earlier and more pronounced RER reductions during light phases (Fig. 2A). From day 5 after emergence onward, the diurnal RER was on average 0.31 d^{-1} lower than the nocturnal RER in *aba4* as compared with 0.16 d^{-1} daytime reduction in the wild type. Contrasting with *aba4*, stomatal conductance was strongly reduced in *NCED6*-OE and, still in line with our hypothesis, it displayed a strongly altered RER pattern (Fig. 2A). Leaf expansion during days was essentially maintained similar to night RER at 5 d following emergence (only 0.01 d^{-1} lower on average). To ascertain the hydraulic origin of growth limitation in the daytime, we exposed both Col-0 and Ws-3 accessions to two levels of soil water deficit. Applying a moderate soil water deficit (0.23 $g_{water}\ g^{-1}{}_{dry\ soil}$) to Col-0 (Fig. 2C) or Ws-3 (Fig. 2D) amplified the diurnal depressions (0.37 d^{-1} lower RER during days than during nights after 5 d), with day drops occurring earlier than under well-watered conditions. Under severe deficit (0.18 $g_{water}\ g^{-1}{}_{dry\ soil}$), diurnal reductions in RER were even more pronounced, especially in Col-0, where leaf expansion virtually ceased during days (0.30 d^{-1} lower RER in the daytime at any developmental stage). By contrast, when the vapor pressure deficit (VPD) was lowered (down to 0.3 kPa instead of 0.8 kPa) in order to improve the leaf water status, day/night alternations of leaf expansion were minimized, with a flattened pattern in the early stages and a diurnal RER being only 0.08 d^{-1} lower than during the night after 5 d on average (Fig. 2B).

Overall, the consistency of the results obtained using stomatal mutants, low evaporative demand, or soil water deficit treatments strongly supports the hypothesis that diurnal reductions in leaf expansion observed during the later phases of leaf development in the well-watered wild-type plants are under hydraulic control. Besides acting on stomatal closure, altered ABA content in stomatal mutants could have imposed long-term additional effects, for instance on hydraulic conductivity, possibly through changes in aquaporin expression, as well as on nonhydraulic processes such as cell wall properties or cell division (for review, see Tardieu et al., 2010). These side effects, together with the slightly but significantly lower net photosynthesis (Fig. 2A, inset), could partly explain the globally lower RER in *NCED6*-OE plants compared with other genotypes.

Night Depressions Are Linked to a Metabolic Control of Leaf Expansion: Evidence from Starch Mutants

Using a similar combination of environmental and genetic approaches, we tested if early nocturnal depressions of growth were due to a carbon limitation. In line with this hypothesis, experiments at elevated CO_2 have suggested that leaf growth is source limited at night (Grimmer and Komor, 1999; Rasse and Tocquin, 2006). As the starch pool is the main carbon source at night in Arabidopsis, we used four mutants with impaired ability to store starch or to use it at night. The starchless *phosphoglucomutase* (*pgm*) mutant cannot synthesize starch (Caspar et al., 1985), whereas the starch accumulator *starch excess1* (*sex1*) is not able to

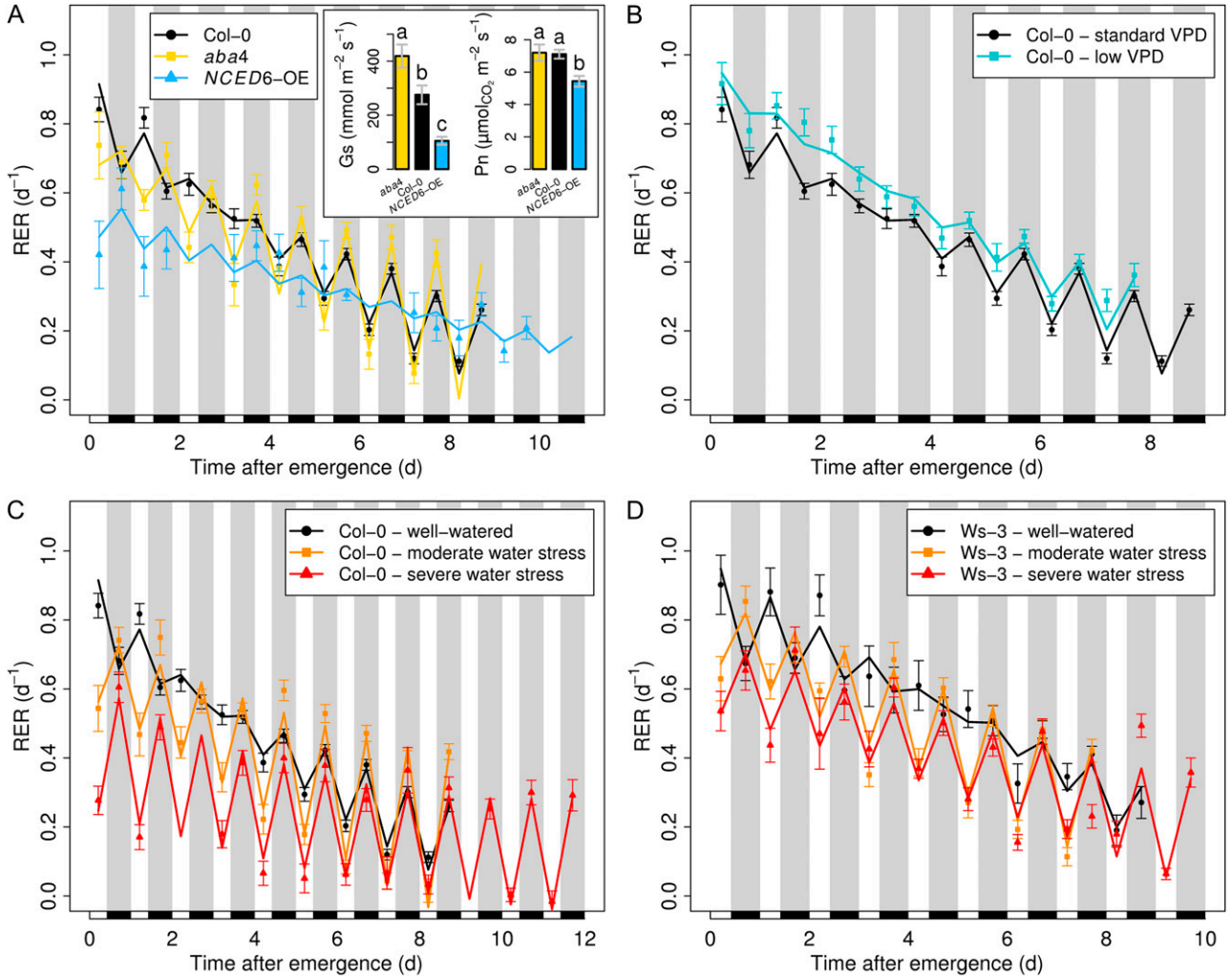

Figure 2. Effects of hydraulic changes on expansion patterns. Points represent observed and lines represent smoothed values. Black rectangles and gray bands indicate the night periods. Values shown are means ± SE ($n \geq 10$). A, Kinetics of stomatal mutants. Expansion patterns are shown for *aba4*, a mild ABA-deficient mutant, and of *NCED6*-OE, an ABA overaccumulator. The inset shows stomatal conductance (Gs) and net photosynthesis (Pn). Letters indicate significant differences between genotypes after a Kruskal-Wallis test. Diurnal stomatal conductance of mutants was affected as expected ($n = 10$). Net photosynthesis was only slightly affected in the overaccumulator ($n = 4$). B, Effects of low VPD on the expansion pattern of Col-0. Well-watered Col-0 was grown either under standard VPD (0.8 kPa during the day; black) or low VPD (0.3 kPa during the day; turquoise). C and D, Kinetics of water-stressed plants. Expansion patterns are shown for Col-0 (C) and Ws-3 (D) plants subjected to a mild water deficit (0.23 $g_{water}\ g^{-1}_{dry\ soil}$) or a severe water deficit (0.18 $g_{water}\ g^{-1}_{dry\ soil}$) and the well-watered control (0.35 $g_{water}\ g^{-1}_{dry\ soil}$). Note the amplification of diurnal depressions under conditions limiting water availability (*aba4*; water stresses) and their diminution when water loss by transpiration is reduced (*NCED6*-OE; low VPD).

degrade it (Caspar et al., 1991). Maltose, the major product of starch breakdown at night, cannot exit the chloroplast in *maltose excess1* (*mex1*; Niittylä et al., 2004). Finally, maltose cytosolic metabolism is impaired in *disproportionating enzyme2* (*dpe2*; Chia et al., 2004; Lu and Sharkey, 2004). As a result, starch turnover was strongly affected in these mutants (Fig. 3, A and B, insets). Strikingly, all mutations caused a strong reduction of leaf expansion at night (Fig. 3, A and B), especially in the early stages, with RER during the first 3 d following emergence being 0.80, 0.58, 0.49, and 0.48 d^{-1} lower at night than in daytime for *pgm*, *sex1*, *mex1*, and *dpe2*, respectively. By comparison, early reductions in RER at night for Col-0 and Ws-3 were only 0.15 and 0.23 d^{-1} lower than daytime RER. Later on during leaf development, the differences between wild-type plants and starch mutants tended to vanish.

This strongly supports the hypothesis that early night reductions in leaf expansion in the wild-type plants are under metabolic control. Amplified growth inhibitions during the night in the starch mutants could have resulted either from the lack of carbon or the triggering of the signaling cascade associated with low levels of sugars (Smith and Stitt, 2007). By con-

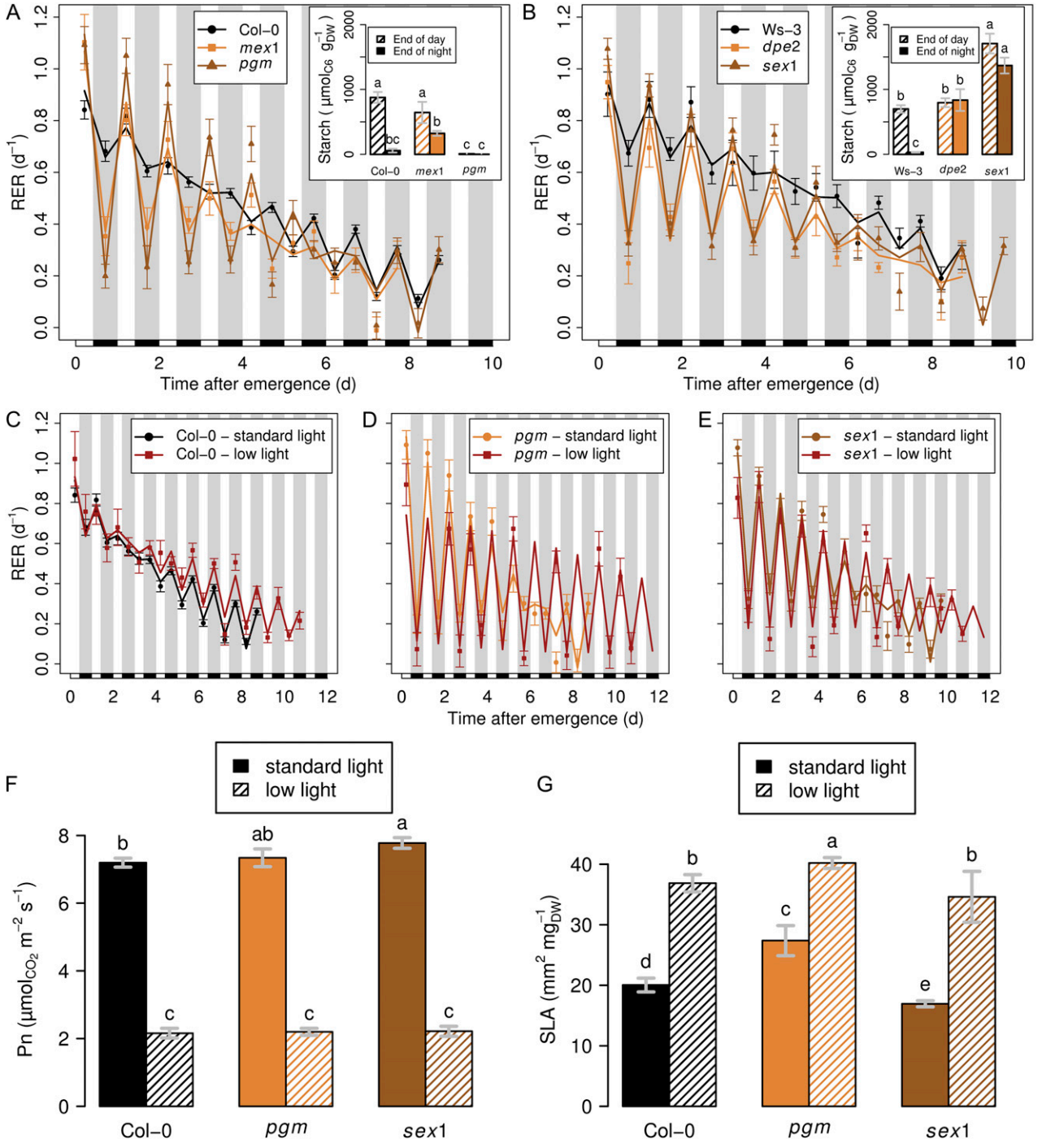

Figure 3. Effects of metabolic changes on expansion patterns. Points represent observed and lines represent smoothed values. Black rectangles and gray bands indicate the night periods. Values shown are means ± SE ($n \geq 10$). A and B, Kinetics of starch mutants. A, Expansion patterns of *pgm*, a starchless mutant, and of *mex1*, a mutant impaired in maltose export (the predominant route for carbohydrate supply at night), both in the Col-0 background. B, Expansion patterns of *sex1*, a starch accumulator, and of *dpe2*, which is affected in the conversion from maltose to Suc at night, both in the Ws-3 background. Insets show starch turnover. The starch content (in μmol of hexose equivalents per unit of dry weight [DW]) was measured at the end of the day and at the end of the night. Letters indicate significant differences between values after a LSD test adjusted using the Bonferroni method ($n = 4$). C to E, Kinetics of plants under low light. Expansion patterns are shown for Col-0 (C), *pgm* (D), and *sex1* (E) subjected to low light (PPFD at 70 μmol m^{-2} s^{-1} versus 220 μmol m^{-2} s^{-1} for the control). F, Effect of irradiance on net photosynthesis (Pn). Letters indicate significant differences between treatments after a Kruskal-Wallis test ($n = 6$). G, Effect of irradiance on SLA. Letters indicate significant differences between treatments after a Kruskal-Wallis test ($n = 4$). Note the amplification of early nocturnal depressions in starch mutants, further increased under low light. The weak effect on the wild type is discussed in the text.

trast, wild-type plants develop buffer systems against carbon starvation, such as described in the whole rosette of Col-0, whose carbon budget is adjusted during the day to avoid exhaustion during the dark period (Gibon et al., 2004, 2009; Bläsing et al., 2005).

Buffering Carbon Starvation

Under very low light (30 μmol m^{-2} s^{-1}), leaf expansion in wild-type Arabidopsis has been shown to be reduced at night (Wiese et al., 2007), but that study did not consider the influence of leaf ontogeny. To further challenge the hypothesis of a carbon limitation of leaf expansion during the early stages of leaf development, Col-0, *pgm*, and *sex1* were exposed to low-light conditions (70 μmol m^{-2} s^{-1}) for 4 d. Surprisingly, this low-light treatment had no effect on the growth pattern of Col-0 (Fig. 3C) during the early stages compared with standard light (220 μmol m^{-2} s^{-1}). At later stages, low light tended to increase the expansion rate, but night RER was still higher than day RER by 0.16 d^{-1} as under standard light. By contrast and as expected, starch mutants (Fig. 3, D and E) under low light displayed throughout development a further decrease of night RER compared with standard light, while daytime RER was increased at later stages as in the wild type. These results raise the question on how the wild type managed to maintain leaf expansion despite severe light reduction. Decreasing the light by two-thirds lowered net assimilation rate by a similar proportion (Fig. 3F), but the specific leaf area (SLA) nearly doubled under low light (Fig. 3G). This implies that the plant essentially maintained surface expansion despite lower carbon availability by adjusting leaf thickness or density. An increase in SLA under low light is classically observed in a variety of species and a wide range of conditions, including species in natural habitats (Boardman, 1977), crop plants (Tardieu et al., 1999), or Arabidopsis (Pigliucci and Kolodynska, 2002; Cookson and Granier, 2006). Similarly in tobacco (*Nicotiana tabacum*), SLA and carbon contribution to structural weight adjusted to photosynthetic capacity (Fichtner et al., 1993). Starch dynamics could also have adjusted in response to the carbon balance, as demonstrated under various daylengths (Gibon et al., 2004, 2009) and under low irradiance (Chatterton and Silvius, 1981). Together, our results fit with the general view that plants use an arsenal of responses allowing them to fine-tune the balance between surface expansion and structural growth. This ability to optimize light interception under limited irradiance by reducing the carbon investment per unit of leaf area (i.e. prioritizing surface expansion) represents a strong ecological advantage (Poorter et al., 2009). Our study also suggests that buffering systems against carbon fluctuations are more efficient in maintaining leaf expansion under carbon-limiting conditions than the mechanisms responsible for attracting water to growing cells when competition for water is high. This makes sense because maintaining surface expansion represents an advantage under low light and a disadvantage under water stress, with respect to photosynthesis and transpiration, respectively. How this response is achieved is not known. Nevertheless, very efficient buffering systems are acting to prevent carbon starvation, redirect gene expression, and slow down growth (Smith and Stitt, 2007). These buffering systems for carbon are likely to be mediated by sugar sensing (Smith and Stitt, 2007; Stitt et al., 2007) and to rely on short-term pool dynamics (e.g. starch; Gibon et al., 2004, 2009) or on long-term changes in carbon investments into structures (Boardman, 1977; Poorter et al., 2009), as seen in our study through a much higher SLA in the leaves of shaded plants. Under more drastic carbon conditions, as in starch mutants (this study) or under very low light (Wiese et al., 2007), limited carbon availability may ultimately impact leaf expansion.

Severe Water Stress Restores the Wild-Type Phenotype in Starch Mutants

To evaluate the possible interactions between carbon and hydraulic limitations, we exposed the starch mutants to soil water deficits. In all mutants, a severe water deficit resulted in a strongly reduced expansion during day phases and a practically unaltered expansion during nights. As a result, all mutants displayed a pattern that resembled that of the well-watered wild-type plants (Supplemental Fig. S4). This is consistent with the superimposition of the gradual influence of hydraulic limitations in the daytime over the growth pattern of starch mutants, characterized by night reduction of RER. Additionally, besides penalizing the hydraulic status, drought could also have improved the carbon status of the starch mutants. This interpretation is in line with a recent review (Muller et al., 2011) showing that drought improves the carbon status of plants due to a higher sensitivity to drought for leaf growth than for carbon assimilation, leading to carbon accumulation (for an exemplification in Arabidopsis, see Hummel et al., 2010). On the whole, the ability to restore qualitatively the wild-type phenotype with starch mutants under water stress indicates that expansion patterns, including those of the wild-type plants, result from a dynamic and plastic combination of metabolic and hydraulic constraints.

A Developmental Switch from Metabolic Limitations to Hydraulic Limitations of Leaf Expansion

In order to analyze the whole data set within a common statistical procedure, expansion patterns were normalized according to the time axis and a clustering was performed based on the difference between night and day RERs, as computed by fitting a polynomial independently to the day and night values (Fig. 4A). The statistical significance of this difference for each treatment at each time step is plotted in Figure 4B. Vertically, this clustering resulted in an ordered continuum of genotypic and environmental conditions lead-

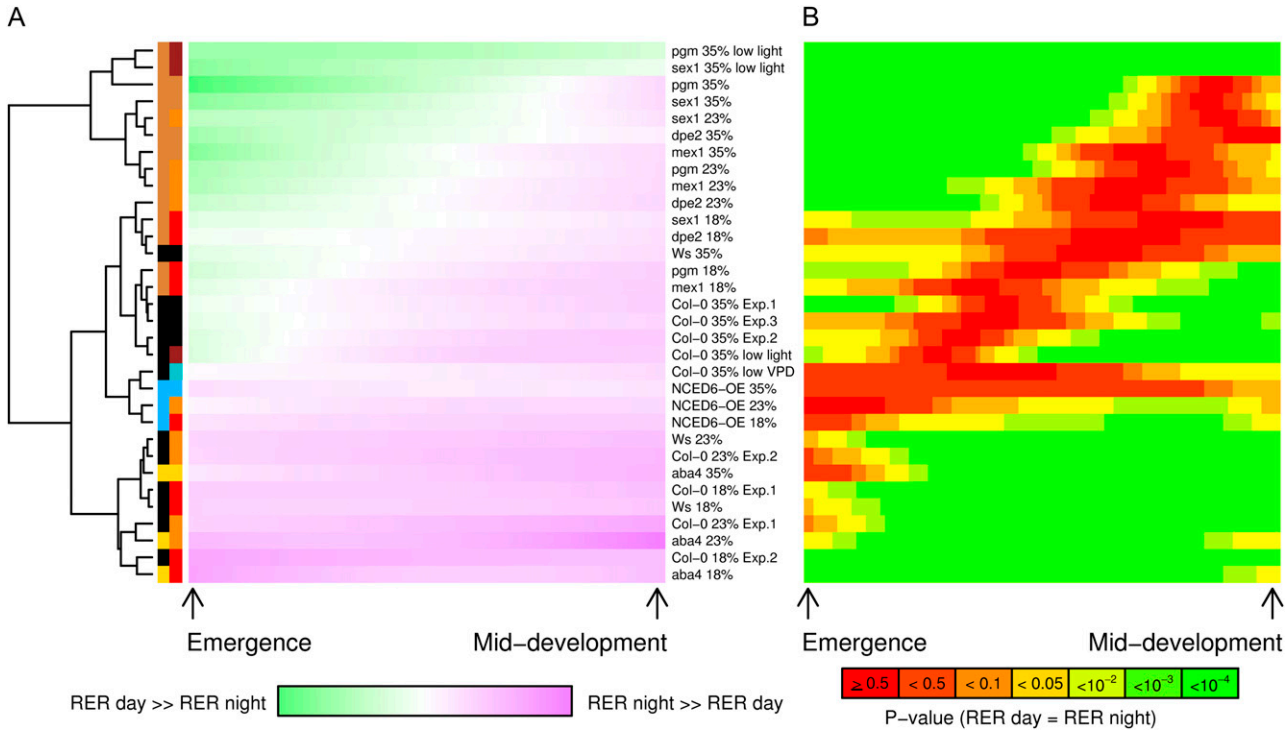

Figure 4. Heat map of the expansion patterns. A, Hierarchical clustering analysis of the difference between night and day RER. The time axis of all kinetics was normalized according to leaf mid development (t_{50}). Then, a second-degree polynomial was fitted independently to the day and night RERs, and the difference between night and day was computed for 100 successive iterations between t_0 (emergence) and t_{50}. These 100 variables were used to classify the kinetics using the Euclidean distances. The computed variables were then associated with a color. Closeness to green indicates a day RER superior to the night RER, while closeness to purple indicates the opposite. The left part of the rectangles beside branches of the dendrogram is a color code for the genotype, while the right part is for the environment. There is no added right part when genotype was grown under control conditions (well watered, standard light). Black is for the wild type. Tan (starch mutants) and brown (low light) are for supposed enhanced metabolic constraints. Gold (*aba4*), orange (moderate water stress), and red (severe water stress) are for supposed enhanced hydraulic constraints. Steel blue (*NCED6*-OE) and turquoise (low VPD) are for supposed reduced hydraulic constraints. Note that mutants and environmental treatments supposed to modify metabolic or hydraulic constraints clustered in a consistent way. Note also that metabolic constraints are predominantly associated with early, nocturnal RER depressions, whereas hydraulic constraints are associated with later, diurnal RER depressions. B, Significance of the difference between night and day RER. Confidence intervals of the polynomial regressions were calculated at several confidence levels for each iteration. Green indicates that the difference between night and day RER is very highly significant, while red indicates no significant difference.

ing to situations ranging from predominant night depressions (top of Figure 4A in green) to predominant day depressions (bottom of Figure 4A in purple) during leaf development. Consistent with our analysis linking night depressions to metabolic constraint, all starch mutants under well-watered or moderate water stress conditions (except *dpe2*) clustered in the top part of Figure 4A, with highly significant night reductions of RER extending several days after leaf emergence. *pgm* and *sex1* under low light were ranked at the upper extreme of the clustering. Under severe water deficit, growth patterns of all starch mutants shifted down within the group of their well-watered wild types, in both Col-0 and Ws-3 backgrounds. Leaf expansion of *NCED6*-OE was poorly affected by water shortage and clustered at any soil water content with the low VPD treatment, forming a group characterized by weak, nonsignificant day/night fluctuations of expansion associated with probable low fluctuations of transpiration. The last group, located at the bottom of the cluster, with strong, highly significant depressions of daytime RER, was composed of all genetic (*aba4* mutant) or environmental (soil water deficits) situations that increased hydraulic limitation. The horizontal color gradient clearly indicated that night depressions occurred preferentially in the early stages whereas day depressions were more pronounced in the later stages, with a switching point (white and red diagonals in Fig. 4, A and B, respectively) following the balance between metabolic and hydraulic constraint. As a whole, the consistent ranking of this clustering gathered from environmental and genetic perturbations shows that during the course of ontogeny, the control of leaf expansion switches from metabolics to hydraulics.

These results imply that even under well-watered conditions, leaf expansion becomes more and more

limited by water fluxes as the leaf develops. Water supply to the growing tissues, therefore, appears as a key point to balance the increasing competition for water between growth and transpiration as the leaf expands. The impact on growth of this competition has been well documented in monocots but also in dicots such as sunflower (Boyer, 1968), castor bean (*Ricinus communis*; Poiré et al., 2010a), and several halophytic species (Rozema et al., 1987). However, to our knowledge, our study is the first one reporting a progressive establishment of hydraulic constraint on leaf growth during its ontogeny. An increasing hydraulic constraint during development could be mediated by various means. First, xylem architecture could become limiting due to a decreased vein density as the leaf expands, as recently reported in Arabidopsis (Rolland-Lagan et al., 2009). Moreover, hydraulic conductivity could decrease with tissue maturation, as shown along fescue leaves (Martre et al., 2000, 2001; Martre and Durand, 2001) and in developing leaves of horsechestnut (*Aesculus hippocastum*; Nardini et al., 2010). Alternatively, aquaporin-mediated water transport may become gradually limiting, as suggested in the maize leaf from the spatial pattern of transcription levels along the maturation zone (Hachez et al., 2008). The global lengthening of the extravascular pathway as the leaf expands may also exert an increasing resistance to water flow within the whole leaf (Cochard et al., 2004; Brodribb et al., 2007). Lastly, stomata dynamics and sensitivity to ABA could be dependent on leaf age, as suggested in cotton (*Gossypium hirsutum*; Jordan et al., 1975). However, the developmental pattern of stomatal or xylem functioning remains unknown for the growing leaves of Arabidopsis.

As a first insight into the mechanisms underlying a hydraulic developmental switch, we determined turgor in young (1 d after emergence) and older (8 d) leaves in well-watered Col-0 at the end of both day and night. Leaf turgor increased with development (Fig. 5A), which fits with earlier observations in maize (Tang and Boyer, 2002; Bouchabké et al., 2006). In those studies, this was attributed either to a depression of water potential induced by the volumetric growth or to changes in rheological parameters with leaf development. More interestingly, our results also showed a clear developmental switch in the day/night turgor difference: just after emergence, turgor was significantly lower at night (0.31 MPa during the day versus 0.18 MPa at night; $P < 0.05$), while a significant drop in turgor was observed during the day at the later stage (0.44 MPa during the day versus 0.56 MPa at night; $P < 0.01$). Similar drops in daytime turgor were recently reported in Arabidopsis leaves using a patch-pressure technique (Ache et al., 2010). Our study suggests that very young leaves are not subjected to this daytime drop and that this developmental switch in the day/night turgor could be involved in the developmental switch in the day/night leaf expansion.

When the clustering was restricted to the first third of the kinetics (e.g. 3 d following emergence for the wild-type plants under control conditions), wild-type plants clustered foremost with the starch mutants (Supplemental Fig. S5). This implies that leaf growth sensitivity to metabolic control occurs in the early, presumably heterotrophic stages. Accordingly, leaf expansion sensitivity to shading in maize (Ben-Haj-Salah and Tardieu, 1996; Muller et al., 2001), sunflower (Granier and Tardieu, 1999; Tardieu et al., 1999), or Arabidopsis (Cookson and Granier, 2006) was enhanced in the young leaf. In sink organs, the growth pattern was also altered at night, as shown for Arabidopsis roots (Yazdanbakhsh and Fisahn, 2010) or potato (*Solanum tuberosum*) internodes (Kehr et al., 1998). Furthermore, close relationships between local carbohydrate availability and growth rate observed in several sink organs support the view that growth dependence upon carbon is an emergent feature of

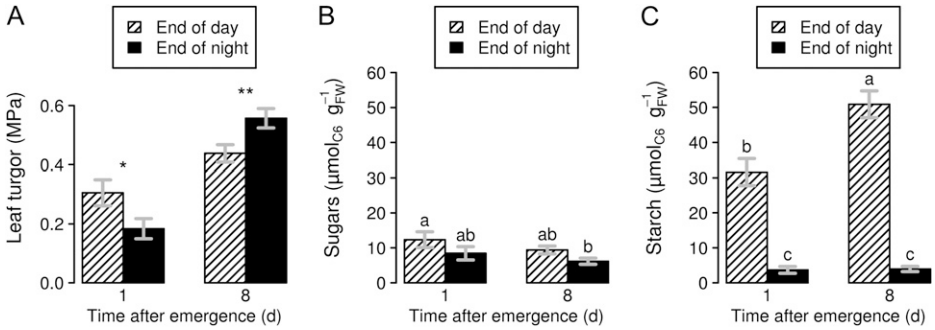

Figure 5. Ontogenetic shifts in leaf turgor and carbohydrate stores. Measurements were performed at the end of day and night on leaves aged 1 and 8 d after emergence on the well-watered Col-0 plants. Values shown are means ± SE. A, Leaf turgor. Turgor pressure was determined as the difference between leaf water potential and osmotic potential. Mean, SE, and ABC confidence interval were computed using a nonparametric bootstrap method. Single and double asterisks indicate significant differences between day and night turgor at the 0.95 and 0.99 confidence levels, respectively. B and C, Carbohydrate stores. The soluble sugar (B) and starch (C) contents were measured (in μmol of hexose equivalent per unit of fresh weight [FW]) at the end of day and night. Letters indicate significant differences between values after a Kruskal-Wallis test ($n \geq 6$).

sink organs (Muller et al., 2011). Thus, the predominance of carbon limitation at leaf emergence and its disappearance during leaf development could be linked to a progressive sink-to-source transition. In several dicots, the sink-to-source transition (the moment when the leaf becomes a net carbon exporter) has been shown to take place when the leaf is 30% to 60% fully expanded, but this view has not been revisited for a long while (for review, see Turgeon, 1989). As far as we know, the impact of sink-to-source balance on patterns of leaf expansion has never been demonstrated. The young leaf must rely on carbohydrate import from older leaves, because its metabolic requirements are maximal when its production capacity is minimal (Turgeon, 1989). Indeed, while photosynthetic machinery is developing (Dale, 1985), relative expansion rate and relative cell division rate are at their highest levels (Cookson and Granier, 2006), increasing carbon needs for respiration (Dale, 1985) and carbon costs such as those associated with the synthesis of new structural compounds and cell equipment, including walls, nucleic acids, and proteins (Piques et al., 2009). Recent transcriptomic data along a developmental gradient in maize leaf support this interpretation (Li et al., 2010). This is also exemplified in the study of Schurr et al. (2000), where the young leaves of castor bean showed a low chlorophyll content, a negative net assimilation rate, and an intense respiration rate, while leaf growth rate was reduced at night.

To evaluate if leaf carbon budgets could be affected by ontogeny, we measured carbohydrate stores of young (1 d after emergence) and older (8 d) leaves in well-watered Col-0 at the end of day and night. Soluble sugar contents (Fig. 5B) were not significantly different between the end of the day and the end of the night. Starch content (Fig. 5C) at the end of the day was three to four times that of soluble sugars and was almost exhausted at the end of the night, suggesting that starch is a major contributor to the leaf diurnal carbon balance. Interestingly, the amount of starch stored at the end of the day in the just emerged leaf was 40% lower than in the older leaf. The carbohydrate stores at the end of the day were thus lower in the young leaf despite its maximal growth rate, which fits with the idea of a steeper metabolic constraint in the young leaf.

Besides hydraulics and metabolics, the circadian clock may play an intertwined role in the control of leaf growth. Recently, it was found that under extended light, leaf expansion rate at a short time scale in Arabidopsis keeps on alternating with a similar period as under normal day/night conditions (Poiré et al., 2010b), highlighting a circadian control of leaf expansion. The developmental switch of the day/night pattern presented in this study and its modulation provide evidence that ontogeny, genetics, and the environment can all overcome endogenous rhythms. The extent to which the clock could interfere with our results is not the scope of this study, but we hypothesize that circadian rhythm could act to amplify and anticipate leaf response, notably to metabolic or hydraulic constraints. Indeed, the clock has been shown to orchestrate the transcription of pathways related to central processes, including photosynthesis, carbon metabolism, or water influx through aquaporins, together with cell wall dynamics (Harmer et al., 2000). Furthermore, sugars themselves can modify the expression of clock-regulated genes (Bläsing et al., 2005), while conversely, starch breakdown is under circadian control (Graf et al., 2010). Stomatal conductance and photosynthesis are also subject to a partial circadian control in Arabidopsis (Dodd et al., 2005). Recently, it was shown that water dynamics as well as aquaporin gene expression in Arabidopsis roots oscillated with the circadian rhythm (Takase et al., 2011). Finally, root xylem pressure (Henzler et al., 1999) and leaf hydraulic conductance (Nardini et al., 2005) have been shown to be clock dependent. Thus, we raise the hypothesis that the influence of the clock on the dual patterns reported here, although not excludable, could be at least partly integrated with the metabolic and hydraulic processes discussed above.

CONCLUSION

Whether carbon or water is the main limitation of leaf growth is a matter of debate in the literature. Here, we provide genetic and environmental evidence that the control of leaf expansion switches from metabolics to hydraulics during the course of leaf ontogeny in Arabidopsis. We demonstrate that this developmental switch is associated with consistent ontogenetic changes in day/night leaf turgor and starch availability. Carbon influence on leaf expansion occurs mainly at night during the early phases of leaf development, maybe due to a limited local starch availability with respect to an intense carbon demand, and is buffered by fine-tuning structural growth. These adjustments maintain surface expansion (and thus energy capture) under limiting light conditions, partly uncoupling leaf expansion from carbon availability. By contrast, as the leaf develops, hydraulics exert increasing constraint during the daytime by altering leaf turgor. To our knowledge, the establishment of an increasing water limitation of leaf growth has not been reported before. Although of yet unknown nature, these limitations could be due to a decreasing capacity of the hydraulic network to supply water to the growing tissues. To what extent this developmental switch can be extrapolated to other species remains an open question. The sink-to-source transition of leaves is a general feature in plants. If this transition is the cause of the weakening of metabolic constraint on leaf expansion, it is tempting to speculate that this response is conserved across species. By contrast, if the ontogenetic establishment of hydraulic constraint on leaf expansion is related to the hydraulic network architecture, which is highly variable across species, the level of hydraulic constraint on leaf expansion is expected to be species

dependent. A superimposition of molecular and physiological information during leaf development to the growth kinetics reported here is now required to further decipher the concerted actions of carbon and water on leaf expansion.

MATERIALS AND METHODS

Growth Conditions

Seeds of Arabidopsis (*Arabidopsis thaliana*) were sown in pots filled with a mixture (1:1, v/v) of loamy soil and organic compost. Once germinated, they were grown in growth chambers at a 10-h photoperiod under a photosynthetic photon flux density (PPFD) of 220 μmol m^{-2} s^{-1}. Air temperature and VPD were 21°C and 0.8 kPa, respectively, during the day and 17°C and 0.3 kPa at night. Each pot was weighed twice a day and watered with one-tenth-strength Hoagland solution, so that its soil water content was maintained at a well-watered level (0.35 g_{water} $g^{-1}_{dry\ soil}$) equivalent to a predawn water potential of −0.3 MPa (Hummel et al., 2010). When plants had 10 visible leaves, irrigation was suspended for the plants exposed to water stress, until soil water content reached a target value corresponding to a mild water deficit (0.23 g_{water} $g^{-1}_{dry\ soil}$, −0.7 MPa) or a severe water deficit (0.18 g_{water} $g^{-1}_{dry\ soil}$, −1.1 MPa). First measurements occurred when the soil water content had stabilized to the target value for 4 d. For the low-VPD experiment, the target VPD was maintained at 0.3 kPa during the day and 0.1 kPa at night from 4 d before the beginning of measurements. For the low-light treatment, a neutral shading veil reduced PPFD to 70 μmol m^{-2} s^{-1}, beginning also 4 d before measurements.

Plant Material

The *aba4* mutant is impaired in neoxanthin synthesis and displays a mild phenotype compared with other ABA-deficient mutants, as ABA can be produced by an alternative pathway (North et al., 2007). By contrast, *NCED6*-OE overexpresses a 9-cis-epoxycarotenoid dioxygenase leading to ABA over-accumulation (Lefebvre et al., 2006). The starchless mutant *pgm* lacks the plastid phosphoglucomutase (Caspar et al., 1985). By contrast, the *sex1* mutant (Caspar et al., 1991) accumulates a large amount of starch, as it is impaired in an α-glucan water dikinase involved in the early steps of starch breakdown (Ritte et al., 2002). The *mex1* mutant is impaired in a maltose transporter at the chloroplast envelope, which represents the predominant route for carbohydrate export from chloroplasts at night (Niittylä et al., 2004). The *dpe2* mutant is affected in the cytosolic disproportionating enzyme involved in the conversion from maltose to Suc at night (Chia et al., 2004; Lu and Sharkey, 2004). All mutants were in the Col-0 background (N1092), except *sex1* and *dpe2*, which were in the Ws-3 background (N1638). Accordingly, both accessions were used in our experiments.

Monitoring Leaf Growth at the Day/Night Time Scale

In order to evaluate leaf growth limitations during its development (which can last more than 1 month; Aguirrezabal et al., 2006) regardless of whole plant changes like floral transition (Christophe et al., 2008), we developed an approach where the expansion of serial leaves over one diurnal and one nocturnal phase is used to infer the expansion of a reconstructed leaf over successive days. Our approach, justified in Supplemental Materials and Methods S1 and fully described in Supplemental Figures S1 to S3, consisted of three consecutive zenithal photographs: the first one at the beginning of a day period, the second one at the end of the same day period, and the third one at the end of the subsequent night. This was repeated 3 d later under maintained environmental regimes as a replicate. During each acquisition, photographs were taken within less than 15 min utilizing the phenotyping automaton developed by our group (Granier et al., 2006). We extracted the area of successive leaves from the digital photographs using a semiautomated program developed on the ImageJ software (Rasband, 2009). The last digitalized leaf was chosen to represent more than half of the area of the largest visible mature leaf (e.g. 13 leaves in the well-watered Col-0). When appropriate, a series of independent photographs was taken to consider hyponasty and the area of each leaf was corrected for its angle (Supplemental Fig. S3). For each leaf rank, the RER was computed as the local slope of the natural logarithm of the area (S) as a function of thermal time to correct for the linear effects of temperature (Granier et al., 2002) and recalculated at a reference temperature of 20°C, as mostly encountered in the literature (Supplemental Fig. S1, step 5). Hence, the diurnal (respectively nocturnal) RER between ti, the beginning of the day (respectively night), and tj, the end of the day (respectively night), was computed as follows:

$$\mathrm{RER}_{ti-tj} = \frac{\ln\left(\frac{S_j}{S_i}\right)}{\int_{ti}^{tj}(T - T_{base})\cdot dt} \times (T_{ref} - T_{base})$$

where T is the temperature, T_{base} is the base temperature of 3°C, and T_{ref} is the reference temperature (set at 20°C). RER was expressed in mm^2 mm^{-2} d^{-1} at 20°C (noted d^{-1} elsewhere in the text). When calculated over 24-h intervals, the daily RER continuously decreased as a function of time, meaning that leaf area increase was always less than exponential, in line with the sigmoid pattern of daily evolution of leaf area (Supplemental Fig. S1, step 3).

The phyllochron of each genotype × environment combination was deduced from leaf number counts (see below). The age of each leaf from its emergence was then computed as:

$$\text{age} = \text{phyllochron} \times (\text{leaf rank from the top} - 1) + \text{time delay since first picture}$$

allowing us to gather the serial leaf ranks in a single reconstructed time series. This switch from a spatial pattern to a temporal time course was possible because successive leaves displayed similar features (Groot and Meicenheimer, 2000) during this 10-h photoperiod, which postponed the influence of flowering. The left panel of Supplemental Figure S2A shows the dynamics of leaf emergence for well-watered Col-0, and the double arrow shows the period of the experiment. The right panel of Supplemental Figure S2A shows the associated phyllochron (inverse of leaf emergence rate) and its stability during the period corresponding to the emergence of the oldest digitalized leaf until the day of measurement (double arrow). Supplemental Figure S2B shows for well-watered Col-0 and *pgm* the measured area for a reconstructed leaf against the logistical fitting using the data obtained from a single leaf followed during several days. R^2 values were high and equivalent between the reconstructed and the single leaf (0.905 against 0.935 and 0.917 against 0.896 for Col-0 and *pgm*, respectively). Then, after discretization to provide a day/night representation of the data, second-degree polynomials were independently fitted to the day RER and to the night RER (Fig. 1, inset; Supplemental Fig. S1, step 6), thereby smoothing kinetics and allowing further statistical analyses. The growth patterns were drawn from emergence to half expansion of the leaf (t_{50}) before growth slowed down, involving other processes than the ones analyzed here. t_{50} was determined for each genotype × environment combination after fitting a logistical function (Aguirrezabal et al., 2006) on the night data set, as exemplified in step 3 of Supplemental Figure S1. We proved that under well-watered conditions, the expansion pattern of the reconstructed leaf was very similar to that obtained if one single leaf was followed over 9 d (Supplemental Fig. S2C). There was a tendency for the single leaf to display a smaller RER in the early stages, maybe due to a whole-plant effect (see the difference between the first and last images in both analyses), but the day/night differences were almost conserved and both treatments clustered closely together when the single leaf was introduced in the hierarchical analysis (Supplemental Fig. S2D, thick lines). Using this framework, we were able to observe highly reproducible fluctuations of expansion rates during leaf development in several replicated experiments (Supplemental Fig. S1E).

Physiological Measurements

We characterized mutants or environments by providing hydraulic or metabolic markers measured on fully expanded leaves or on the whole plant. Stomatal conductance was calculated as the sum of the conductances measured on both sides of a fully expanded leaf on 10 replicates using a diffusion porometer (AP4; Δ-T Devices). The net CO_2 assimilation rate was measured with a whole plant chamber designed for Arabidopsis and connected to a gas analyzer (CIRAS-2; PP Systems) on four to six individual plants. SLA was measured as described by Hummel et al. (2010) on four whole rosettes. Starch and soluble sugar (as the sum of Glc, Fru, and Suc) contents were analyzed by enzymatic assay as described by Hummel et al. (2010) using material harvested at the ends of day and night, either on fully expanded leaves of four individual plants (Fig. 3) or on pools of about 50 leaves aged 1 or 8 d that were replicated three times independently and at least twice technically (Fig. 5). Leaf turgor was determined on leaves aged 1 or 8 d at the ends of day and

night as the difference between water and osmotic potential. For water potential measurements, leaves were harvested and immediately inserted in a sealed chamber carrying a thermocouple (C-52; Wescor) connected to a wet bulb depression psychrometer (Psypro; Wescor). A foliar disc was punched for the 8-d-old leaves, which were larger than the 7-mm diameter sample holder. At least 25 replicates were performed. For osmotic potential, a pool of leaves was harvested in liquid nitrogen and stored at −60°C. Samples were then transferred into 0.8-μm filters (NucleoSpin filters; Macherey-Nagel) inserted in a collection tube and centrifuged at 4°C. Samples of 10 μL of the resulting sap (n = 8 for the early stage and n = 48 for the later stage) were analyzed using a vapor pressure osmometer (Vapro 5520; Wescor).

Statistical Analyses

All graphics and statistical analyses were performed with the R software (R Development Core Team, 2008). Mean comparisons were performed with the LSD test adjusted using the Bonferroni method or with the Kruskal-Wallis test when heteroscedasticity was detected.

For the heat map, the time axis of all kinetics was normalized according to their t_{50}. Then, a second-degree polynomial was fitted independently to the day and night RERs, and their difference was computed for 100 successive iterations between t_0 (emergence) and t_{50} to provide a continuous visualization of the difference dynamics. These 100 variables were used for the hierarchical clustering of the kinetics, which was performed with the Euclidean distances. Confidence intervals of the polynomial regressions were calculated at the 0.5, 0.9, 0.95, 0.99, 0.999, and 0.9999 confidence levels for each iteration. The level from which day confidence interval and night confidence interval overlapped set the significance of the difference between day and night RER.

As turgor was determined using two variables measured on independent samples, a nonparametric stratified bootstrap was performed to obtain the mean and SE of the computed variable. The nonparametric approximate bootstrap confidence intervals were then calculated at the 0.9, 0.95, 0.99, and 0.999 confidence levels to evaluate the significance of the difference between day and night at each investigated stage.

Supplemental Data

The following materials are available in the online version of this article.

Supplemental Figure S1. Process from plant images to RER patterns.

Supplemental Figure S2. Validation of the leaf reconstruction method.

Supplemental Figure S3. Taking hyponasty into account.

Supplemental Figure S4. Effect of a severe metabolic and hydraulic constraint in combination.

Supplemental Figure S5. Heat map of the expansion patterns for the first third of the kinetics.

Supplemental Materials and Methods S1. From leaf rank to leaf age: uses and principles.

ACKNOWLEDGMENTS

We thank Samuel Zeeman and Annie Marion-Poll for supplying seeds of starch and ABA mutants, respectively. We are grateful to Nathalie Wuyts for developing the ImageJ program to assist leaf area extraction. Finally, we acknowledge Christophe Maurel and two anonymous reviewers for their suggestions to improve the manuscript.

Received March 12, 2011; accepted April 4, 2011; published April 6, 2011.

LITERATURE CITED

Acevedo E, Hsiao TC, Henderson DW (1971) Immediate and subsequent growth responses of maize leaves to changes in water status. Plant Physiol **48:** 631–636

Ache P, Bauer H, Kollist H, Al-Rasheid KAS, Lautner S, Hartung W, Hedrich R (2010) Stomatal action directly feeds back on leaf turgor: new insights into the regulation of the plant water status from non-invasive pressure probe measurements. Plant J **62:** 1072–1082

Aguirrezabal LAN, Bouchier-Combaud S, Radziejwoski A, Dauzat M, Cookson SJ, Granier C (2006) Plasticity to soil water deficit in Arabidopsis thaliana: dissection of leaf development into underlying growth dynamic and cellular variables reveals invisible phenotypes. Plant Cell Environ **29:** 2216–2227

Aguirrezabal LAN, Deleens E, Tardieu F (1994) Root elongation rate is accounted for by intercepted PPFD and source-sink relations in field and laboratory-grown sunflower. Plant Cell Environ **17:** 443–450

Ben-Haj-Salah H, Tardieu F (1996) Quantitative analysis of the combined effects of temperature, evaporative demand and light on leaf elongation rate in well-watered field and laboratory-grown maize plants. J Exp Bot **47:** 1689–1698

Ben-Haj-Salah H, Tardieu F (1997) Control of leaf expansion rate of droughted maize plants under fluctuating evaporative demand: a superposition of hydraulic and chemical messages? Plant Physiol **114:** 893–900

Bergmann DC, Sack FD (2007) Stomatal development. Annu Rev Plant Biol **58:** 163–181

Bläsing OE, Gibon Y, Günther M, Höhne M, Morcuende R, Osuna D, Thimm O, Usadel B, Scheible W-R, Stitt M (2005) Sugars and circadian regulation make major contributions to the global regulation of diurnal gene expression in *Arabidopsis*. Plant Cell **17:** 3257–3281

Boardman NK (1977) Comparative photosynthesis of sun and shade plants. Annu Rev Plant Physiol **28:** 355–377

Bouchabké O, Tardieu F, Simonneau T (2006) Leaf growth and turgor in growing cells of maize (Zea mays L.) respond to evaporative demand under moderate irrigation but not in water-saturated soil. Plant Cell Environ **29:** 1138–1148

Boyer JS (1968) Relationship of water potential to growth of leaves. Plant Physiol **43:** 1056–1062

Boyer JS (1988) Cell enlargement and growth-induced water potentials. Physiol Plant **73:** 311–316

Brodribb TJ, Feild TS, Jordan GJ (2007) Leaf maximum photosynthetic rate and venation are linked by hydraulics. Plant Physiol **144:** 1890–1898

Brouquisse R, James F, Raymond P, Pradet A (1991) Study of glucose starvation in excised maize root tips. Plant Physiol **96:** 619–626

Caspar T, Huber SC, Somerville C (1985) Alterations in growth, photosynthesis, and respiration in a starchless mutant of *Arabidopsis thaliana* (L.) deficient in chloroplast phosphoglucomutase activity. Plant Physiol **79:** 11–17

Caspar T, Lin TP, Kakefuda G, Benbow L, Preiss J, Somerville C (1991) Mutants of Arabidopsis with altered regulation of starch degradation. Plant Physiol **95:** 1181–1188

Chatterton NJ, Silvius JE (1981) Photosynthate partitioning into starch in soybean leaves. II. Irradiance level and daily photosynthetic period duration effects. Plant Physiol **67:** 257–260

Chia T, Thorneycroft D, Chapple A, Messerli G, Chen J, Zeeman SC, Smith SM, Smith AM (2004) A cytosolic glucosyltransferase is required for conversion of starch to sucrose in Arabidopsis leaves at night. Plant J **37:** 853–863

Christ RA (1978) The elongation rate of wheat leaves. II. Effect of sudden light change on the elongation rate. J Exp Bot **29:** 611–618

Christophe A, Letort V, Hummel I, Cournède P-H, de Reffye P, Lecoeur J (2008) A model-based analysis of the dynamics of carbon balance at the whole-plant level in Arabidopsis thaliana. Funct Plant Biol **35:** 1147–1162

Clifton-Brown JC, Jones MB (1999) Alteration of transpiration rate, by changing air vapour pressure deficit, influences leaf extension rate transiently in Miscanthus. J Exp Bot **50:** 1393–1401

Cochard H, Nardini A, Coll L (2004) Hydraulic architecture of leaf blades: where is the main resistance? Plant Cell Environ **27:** 1257–1267

Cookson SJ, Granier C (2006) A dynamic analysis of the shade-induced plasticity in Arabidopsis thaliana rosette leaf development reveals new components of the shade-adaptative response. Ann Bot (Lond) **97:** 443–452

Cutler JM, Steponkus PL, Wach MJ, Shahan KW (1980) Dynamic aspects and enhancement of leaf elongation in rice. Plant Physiol **66:** 147–152

Dale JE (1985) The carbon relations of the developing leaf. *In* NR Baker, WJ Davies, CK Ong, eds, Control of Leaf Growth. Cambridge University Press, New York, pp 239–266

Dale JE (1988) The control of leaf expansion. Annu Rev Plant Physiol Plant Mol Biol **39:** 267–295

Dodd AN, Salathia N, Hall A, Kévei E, Tóth R, Nagy F, Hibberd JM,

Millar AJ, Webb AAR (2005) Plant circadian clocks increase photosynthesis, growth, survival, and competitive advantage. Science **309:** 630–633

Dosio GAA, Tardieu F, Turc O (2011) Floret initiation, tissue expansion and carbon availability at the meristem of the sunflower capitulum as affected by water or light deficits. New Phytol **189:** 94–105

Durand JL, Onillon B, Schnyder H, Rademacher I (1995) Drought effects on cellular and spatial parameters of leaf growth in tall fescue. J Exp Bot **46:** 1147–1157

Ehlert C, Maurel C, Tardieu F, Simonneau T (2009) Aquaporin-mediated reduction in maize root hydraulic conductivity impacts cell turgor and leaf elongation even without changing transpiration. Plant Physiol **150:** 1093–1104

Fichtner K, Quick WP, Schulze ED, Mooney HA, Rodermel SR, Bogorad L, Stitt M (1993) Decreased ribulose-1,5-bisphosphate carboxylase-oxygenase in transgenic tobacco transformed with "antisense" rbcS. V. Relationship between photosynthetic rate, storage strategy, biomass allocation and vegetative plant growth at three different nitrogen supplies. Planta **190:** 1–9

Freixes S, Thibaud MC, Tardieu F, Muller B (2002) Root elongation and branching is related to local hexose concentration in Arabidopsis thaliana seedlings. Plant Cell Environ **25:** 1357–1366

Gibon Y, Bläsing OE, Palacios-Rojas N, Pankovic D, Hendriks JHM, Fisahn J, Höhne M, Günther M, Stitt M (2004) Adjustment of diurnal starch turnover to short days: depletion of sugar during the night leads to a temporary inhibition of carbohydrate utilization, accumulation of sugars and post-translational activation of ADP-glucose pyrophosphorylase in the following light period. Plant J **39:** 847–862

Gibon Y, Pyl E-T, Sulpice R, Lunn JE, Höhne M, Günther M, Stitt M (2009) Adjustment of growth, starch turnover, protein content and central metabolism to a decrease of the carbon supply when Arabidopsis is grown in very short photoperiods. Plant Cell Environ **32:** 859–874

Graf A, Schlereth A, Stitt M, Smith AM (2010) Circadian control of carbohydrate availability for growth in Arabidopsis plants at night. Proc Natl Acad Sci USA **107:** 9458–9463

Granier C, Aguirrezabal L, Chenu K, Cookson SJ, Dauzat M, Hamard P, Thioux J-J, Rolland G, Bouchier-Combaud S, Lebaudy A, et al (2006) PHENOPSIS, an automated platform for reproducible phenotyping of plant responses to soil water deficit in Arabidopsis thaliana permitted the identification of an accession with low sensitivity to soil water deficit. New Phytol **169:** 623–635

Granier C, Massonnet C, Turc O, Muller B, Chenu K, Tardieu F (2002) Individual leaf development in Arabidopsis thaliana: a stable thermal-time-based programme. Ann Bot (Lond) **89:** 595–604

Granier C, Tardieu F (1999) Leaf expansion and cell division are affected by reducing absorbed light before but not after the decline in cell division rate in the sunflower leaf. Plant Cell Environ **22:** 1365–1376

Grimmer C, Komor E (1999) Assimilate export by leaves of Ricinus communis L. growing under normal and elevated carbon dioxide concentrations: the same rate during the day, a different rate at night. Planta **209:** 275–281

Groot EP, Meicenheimer RD (2000) Short-day-grown Arabidopsis thaliana satisfies the assumptions of the plastochron index as a time variable in development. Int J Plant Sci **161:** 749–756

Hachez C, Heinen RB, Draye X, Chaumont F (2008) The expression pattern of plasma membrane aquaporins in maize leaf highlights their role in hydraulic regulation. Plant Mol Biol **68:** 337–353

Harmer SL, Hogenesch JB, Straume M, Chang HS, Han B, Zhu T, Wang X, Kreps JA, Kay SA (2000) Orchestrated transcription of key pathways in Arabidopsis by the circadian clock. Science **290:** 2110–2113

Henzler T, Waterhouse RN, Smyth AJ, Carvajal M, Cooke DT, Schäffner AR, Steudle E, Clarkson DT (1999) Diurnal variations in hydraulic conductivity and root pressure can be correlated with the expression of putative aquaporins in the roots of Lotus japonicus. Planta **210:** 50–60

Hsiao TC (1973) Plant responses to water stress. Annu Rev Plant Physiol **24:** 519–570

Hummel I, Pantin F, Sulpice R, Piques MC, Rolland G, Dauzat M, Christophe A, Pervent M, Bouteillé M, Stitt M, et al (2010) Arabidopsis plants acclimate to water deficit at low cost through changes of carbon usage: an integrated perspective using growth, metabolite, enzyme, and gene expression analysis. Plant Physiol **154:** 357–372

Jordan WR, Brown KW, Thomas JC (1975) Leaf age as a determinant in stomatal control of water loss from cotton during water stress. Plant Physiol **56:** 595–599

Kehr J, Hustiak F, Walz C, Willmitzer L, Fisahn J (1998) Transgenic plants changed in carbon allocation pattern display a shift in diurnal growth pattern. Plant J **16:** 497–503

Kerstiens G (2006) Water transport in plant cuticles: an update. J Exp Bot **57:** 2493–2499

Lacointe A, Minchin PEH (2008) Modelling phloem and xylem transport within a complex architecture. Funct Plant Biol **35:** 772–780

Lefebvre V, North H, Frey A, Sotta B, Seo M, Okamoto M, Nambara E, Marion-Poll A (2006) Functional analysis of Arabidopsis NCED6 and NCED9 genes indicates that ABA synthesized in the endosperm is involved in the induction of seed dormancy. Plant J **45:** 309–319

Li P, Ponnala L, Gandotra N, Wang L, Si Y, Tausta SL, Kebrom TH, Provart N, Patel R, Myers CR, et al (2010) The developmental dynamics of the maize leaf transcriptome. Nat Genet **42:** 1060–1067

Lockhart JA (1965) An analysis of irreversible plant cell elongation. J Theor Biol **8:** 264–275

Lu Y, Sharkey TD (2004) The role of amylomaltase in maltose metabolism in the cytosol of photosynthetic cells. Planta **218:** 466–473

Martre P, Cochard H, Durand JL (2001) Hydraulic architecture and water flow in growing grass tillers (Festuca arundinacea Schreb.). Plant Cell Environ **24:** 65–76

Martre P, Durand JL (2001) Quantitative analysis of vasculature in the leaves of Festuca arundinacea (Poaceae): implications for axial water transport. Int J Plant Sci **162:** 755–766

Martre P, Durand JL, Cochard H (2000) Changes in axial hydraulic conductivity along elongating leaf blades in relation to xylem maturation in tall fescue. New Phytol **146:** 235–247

Minchin PEH, Thorpe MR, Farrar JF (1993) A simple mechanistic model of phloem transport which explains sink priority. J Exp Bot **44:** 947–955

Monteith JL (1977) Climate and the efficiency of crop production in Britain. Philos Trans R Soc B **281:** 277–294

Muller B, Pantin F, Génard M, Turc O, Freixes S, Piques MC, Gibon Y (2011) Water deficits uncouple growth from photosynthesis, increase C content, and modify the relationships between C and growth in sink organs. J Exp Bot **62:** 1715–1729

Muller B, Reymond M, Tardieu F (2001) The elongation rate at the base of a maize leaf shows an invariant pattern during both the steady-state elongation and the establishment of the elongation zone. J Exp Bot **52:** 1259–1268

Nardini A, Raimondo F, Lo Gullo MA, Salleo S (2010) Leafminers help us understand leaf hydraulic design. Plant Cell Environ **33:** 1091–1100

Nardini A, Salleo S, Andri S (2005) Circadian regulation of leaf hydraulic conductance in sunflower (Helianthus annuus L. cv Margot). Plant Cell Environ **28:** 750–759

Niittylä T, Messerli G, Trevisan M, Chen J, Smith AM, Zeeman SC (2004) A previously unknown maltose transporter essential for starch degradation in leaves. Science **303:** 87–89

North HM, De Almeida A, Boutin JP, Frey A, To A, Botran L, Sotta B, Marion-Poll A (2007) The Arabidopsis ABA-deficient mutant aba4 demonstrates that the major route for stress-induced ABA accumulation is via neoxanthin isomers. Plant J **50:** 810–824

Pigliucci M, Kolodynska A (2002) Phenotypic plasticity to light intensity in Arabidopsis thaliana: invariance of reaction norms and phenotypic integration. Evol Ecol **16:** 27–47

Piques M, Schulze WX, Höhne M, Usadel B, Gibon Y, Rohwer J, Stitt M (2009) Ribosome and transcript copy numbers, polysome occupancy and enzyme dynamics in Arabidopsis. Mol Syst Biol **5:** 314

Poiré R, Schneider H, Thorpe MR, Kuhn AJ, Schurr U, Walter A (2010a) Root cooling strongly affects diel leaf growth dynamics, water and carbohydrate relations in Ricinus communis. Plant Cell Environ **33:** 408–417

Poiré R, Wiese-Klinkenberg A, Parent B, Mielewczik M, Schurr U, Tardieu F, Walter A (2010b) Diel time-courses of leaf growth in monocot and dicot species: endogenous rhythms and temperature effects. J Exp Bot **61:** 1751–1759

Poorter H, Niinemets Ü, Poorter L, Wright IJ, Villar R (2009) Causes and consequences of variation in leaf mass per area (LMA): a meta-analysis. New Phytol **182:** 565–588

R Development Core Team (2008) R: A Language and Environment for Statistical Computing. R Foundation for Statistical Computing, Vienna. http://www.R-project.org

Rasband WS (2009) ImageJ. U.S. National Institutes of Health, Bethesda, MD. http://rsb.info.nih.gov/ij/

Rasse DP, Tocquin P (2006) Leaf carbohydrate controls over Arabidopsis growth and response to elevated CO_2: an experimentally based model. New Phytol **172:** 500–513

Richardson A, Wojciechowski T, Franke R, Schreiber L, Kerstiens G, Jarvis M, Fricke W (2007) Cuticular permeance in relation to wax and cutin development along the growing barley (Hordeum vulgare) leaf. Planta **225:** 1471–1481

Ritte G, Lloyd JR, Eckermann N, Rottmann A, Kossmann J, Steup M (2002) The starch-related R1 protein is an alpha-glucan, water dikinase. Proc Natl Acad Sci USA **99:** 7166–7171

Rolland-Lagan AG, Amin M, Pakulska M (2009) Quantifying leaf venation patterns: two-dimensional maps. Plant J **57:** 195–205

Rozema J, Arp W, Diggelen J, Kok E, Letschert J (1987) An ecophysiological comparison of measurements of the diurnal rhythm of the leaf elongation and changes of the leaf thickness of salt-resistant Dicotyledonae and Monocotyledonae. J Exp Bot **38:** 442–453

Schnyder H, Nelson CJ (1988) Diurnal growth of tall fescue leaf blades. I. Spatial distribution of growth, deposition of water, and assimilate import in the elongation zone. Plant Physiol **86:** 1070–1076

Schurr U, Heckenberger U, Herdel K, Walter A, Feil R (2000) Leaf development in Ricinus communis during drought stress: dynamics of growth processes, of cellular structure and of sink-source transition. J Exp Bot **51:** 1515–1529

Smith AM, Stitt M (2007) Coordination of carbon supply and plant growth. Plant Cell Environ **30:** 1126–1149

Stitt M, Gibon Y, Lunn JE, Piques M (2007) Multilevel genomics analysis of carbon signalling during low carbon availability: coordinating the supply and utilisation of carbon in a fluctuating environment. Funct Plant Biol **34:** 526–549

Sulpice R, Pyl E-T, Ishihara H, Trenkamp S, Steinfath M, Witucka-Wall H, Gibon Y, Usadel B, Poree F, Piques MC, et al (2009) Starch as a major integrator in the regulation of plant growth. Proc Natl Acad Sci USA **106:** 10348–10353

Takase T, Ishikawa H, Murakami H, Kikuchi J, Sato-Nara K, Suzuki H (2011) The circadian clock modulates water dynamics and aquaporin expression in Arabidopsis roots. Plant Cell Physiol **52:** 373–383

Tang AC, Boyer JS (2002) Growth-induced water potentials and the growth of maize leaves. J Exp Bot **53:** 489–503

Tang AC, Boyer JS (2008) Xylem tension affects growth-induced water potential and daily elongation of maize leaves. J Exp Bot **59:** 753–764

Tardieu F, Granier C, Muller B (1999) Modelling leaf expansion in a fluctuating environment: are changes in specific leaf area a consequence of changes in expansion rate? New Phytol **143:** 33–43

Tardieu F, Parent B, Simonneau T (2010) Control of leaf growth by abscisic acid: hydraulic or non-hydraulic processes? Plant Cell Environ **33:** 636–647

Tardieu F, Reymond M, Hamard P, Granier C, Muller B (2000) Spatial distributions of expansion rate, cell division rate and cell size in maize leaves: a synthesis of the effects of soil water status, evaporative demand and temperature. J Exp Bot **51:** 1505–1514

Tardieu F, Tuberosa R (2010) Dissection and modelling of abiotic stress tolerance in plants. Curr Opin Plant Biol **13:** 206–212

Turgeon R (1989) The sink-source transition in leaves. Annu Rev Plant Physiol Plant Mol Biol **40:** 119–138

van den Honert TH (1948) Water transport in plants as a catenary process. Discuss Faraday Soc **3:** 146–153

Walter A, Schurr U (2005) Dynamics of leaf and root growth: endogenous control versus environmental impact. Ann Bot (Lond) **95:** 891–900

Walter A, Silk WK, Schurr U (2009) Environmental effects on spatial and temporal patterns of leaf and root growth. Annu Rev Plant Biol **60:** 279–304

Wiese A, Christ MM, Virnich O, Schurr U, Walter A (2007) Spatio-temporal leaf growth patterns of Arabidopsis thaliana and evidence for sugar control of the diel leaf growth cycle. New Phytol **174:** 752–761

Yazdanbakhsh N, Fisahn J (2010) Analysis of Arabidopsis thaliana root growth kinetics with high temporal and spatial resolution. Ann Bot (Lond) **105:** 783–791

SUPPLEMENTAL MATERIAL

Supplementary methods. From leaf rank to leaf age: uses and principles.

Fig. S1. Process from plant images to RER patterns.

Fig. S2. Validation of the leaf reconstruction method.

Fig. S3. Taking hyponasty into account.

Fig. S4. Effect of a severe metabolic and hydraulic constraint in combination.

Fig. S5. Heatmap of the expansion patterns for the first third of the kinetics.

Supplementary methods. From leaf rank to leaf age: uses and principles.

In order to evaluate leaf growth limitations during its development (that can last more than one month, see Aguirrezabal et al., 2006) regardless of whole plant changes like floral transition (Christophe et al., 2008), we developed an approach, fully described from Fig. S1 to Fig. S3, which consisted in translating the spatial information given by serial leaves at a given instant into a time series. The use of serial leaves of the same shoot to study changes occurring during leaf development has been recommended for long, for instance through the leaf plastochron index (Erickson and Michelini, 1957). Its relevance has been demonstrated in many species, including *Arabidopsis thaliana* grown under short day (Groot and Meicenheimer, 2000b). Ontogeny-dependent variables studied following this spatiotemporal rationale encompass leaf processes as various as expansion under water stress (Silk, 1980; Hsiao et al., 1985), morphological and anatomical changes (Isebrands and Larson, 1973; 1977; Groot and Meicenheimer, 2000a; Taylor et al., 2003), carbon balance (Silvius et al., 1978; Dickson and Larson, 1981; Kennedy and Johnson, 1981; Gagnon and Beebe, 1996; Ade-Ademilua and Botha, 2007; Reich et al., 2009), water relations (Schultz and Matthews, 1993), biomechanics (Niklas, 1991), interactions with pests (Shaik et al., 1989; Kleiner et al., 2003), or even genes expression in Arabidopsis (Efroni et al., 2008). Our method, which is based on the phyllochron age converted into time allowing a day/night representation of the data, assumes the n^{th} leaf of a stem at a given time t_1 is equivalent than the $n^{th} + 1$ older leaf at t_0, provided that $t_1 - t_0$ equals the time required for one leaf to emerge (*i.e.* the phyllochron) between leaf n and n + 1. Literature indicates that this assumption holds true for Arabidopsis rosette at least considered during a period affected neither by germination nor flowering: at 12 h photoperiod, expansion duration of successive leaves is almost constant while leaf emergence proceeds at a stable rate (Cookson et al., 2007); even at 16 h photoperiod, RER dynamics of all the 10 leaves non-preformed in the seed fitted a unique relationship (Chenu et al., 2005); above all, similar RERs and steady plastochrons were observed for more than 25 successive leaves at the 10 h photoperiod where vegetative period is extended (Groot and Meicenheimer, 2000b). We used the latter short day photoperiod and validated the assumption in our control conditions at several levels, including phyllochron, leaf area, and RER (see Fig. S2).

References cited in this section

Ade-Ademilua OE, Botha CEJ (2007) Sink to source transition in Pisum sativum leaves in relation to leaf plastochron index. Am J Plant Physiol **2**: 27-35

Aguirrezabal LAN, Bouchier-Combaud S, Radziejwoski A, Dauzat M, Cookson SJ, Granier C (2006) Plasticity to soil water deficit in Arabidopsis thaliana: dissection of leaf development into underlying growth dynamic and cellular variables reveals invisible phenotypes. Plant, Cell Environ **29**: 2216-2227

Chenu K, Franck N, Dauzat J, Barczi J-F, Rey H, Lecoeur J (2005) Integrated responses of rosette organogenesis, morphogenesis and architecture to reduced incident light in Arabidopsis thaliana results in higher efficiency of light interception. Funct Plant Biol **32**: 1123-1134

Christophe A, Letort V, Hummel I, Cournède P-H, Reffye P de, Lecoeur J (2008) A model-based analysis of the dynamics of carbon balance at the whole-plant level in Arabidopsis thaliana. Funct Plant Biol **35**: 1147-1162

Cookson SJ, Chenu K, Granier C (2007) Day length affects the dynamics of leaf expansion and cellular development in Arabidopsis thaliana partially through floral transition timing. Ann Bot **99**: 703-711

Dickson RE, Larson PR (1981) 14C fixation, metabolic labeling patterns, and translocation profiles during leaf development in Populus deltoides. Planta **152**: 461-470

Efroni I, Blum E, Goldschmidt A, Eshed Y (2008) A protracted and dynamic maturation schedule underlies Arabidopsis leaf development. Plant Cell **20**: 2293-2306

Erickson RO, Michelini FJ (1957) The plastochron index. Am J Bot **44**: 297-305

Gagnon M-J, Beebe DU (1996) Establishment of a plastochron index and analysis of the sink-to-source transition in leaves of Moricandia arvensis (L.) DC. (Brassicaceae). Int J Plant Sci **157**: 262-268

Groot EP, Meicenheimer RD (2000a) Comparison of leaf plastochron index and allometric analyses of tooth development in Arabidopsis thaliana. J Plant Growth Regul **19**: 77-89

Groot EP, Meicenheimer RD (2000b) Short-day-grown Arabidopsis thaliana satisfies the assumptions of the plastochron index as a time variable in development. Int J Plant Sci **161**: 749-756

Hsiao TC, Silk WK, Jing J (1985) Leaf growth and water deficits: biophysical effects. In NR Baker, WJ Davies, CK Ong, eds, Control of leaf growth. Cambridge University Press, New York, ppp 239-266

Isebrands JG, Larson PR (1973) Anatomical changes during leaf ontogeny in Populus deltoides. Am J Bot **60**: 199-208

Isebrands JG, Larson PR (1977) Organization and ontogeny of the vascular system in the petiole of eastern cottonwood. Am J Bot **64**: 65-77

Kennedy RA, Johnson D (1981) Changes in photosynthetic characteristics during leaf development in apple. Photosynth Res **2**: 213-223

Kleiner KW, Ellis DD, McCown BH, Raffa KF (2003) Leaf ontogeny influences leaf phenolics and the efficacy of genetically expressed Bacillus thuringiensis cry1A (a) d-endotoxin in hybrid poplar against gypsy moth. J Chem Ecol **29**: 2585-2602

Niklas KJ (1991) The elastic moduli and mechanics of Populus tremuloides (Salicaceae) petioles in bending and torsion. Am J Bot **78**: 989-996

Reich PB, Falster DS, Ellsworth DS, Wright IJ, Westoby M, Oleksyn J, Lee TD (2009) Controls on declining carbon balance with leaf age among 10 woody species in Australian woodland: do leaves have zero daily net carbon balances when they die? New Phytol **183**: 153-166

Schultz HR, Matthews MA (1993) Xylem development and hydraulic conductance in sun and shade shoots of grapevine (Vitis vinifera L.): evidence that low light uncouples water transport capacity from leaf area. Planta **190**: 393-406

Shaik M, Dickinson TA, Steadman JR (1989) Variation in rust susceptibility in beans: predicting lesion size from leaf developmental stage measured by leaf age, length, and plastochron index. Phytopathology **79**: 1035-1042

Silk WK (1980) Plastochron indices in cantaloupe grown on an irrigation line source. Bot Gaz **141**: 73-78

Silvius JE, Kremer DF, Lee DR (1978) Carbon assimilation and translocation in soybean leaves at different stages of development. Plant Physiol **62**: 54-58

Taylor G, Tricker PJ, Zhang FZ, Alston VJ, Miglietta F, Kuzminsky E (2003) Spatial and temporal effects of free-air CO2 enrichment (POPFACE) on leaf growth, cell expansion, and cell production in a closed canopy of poplar. Plant Physiol **131**: 177-185

Figure S1

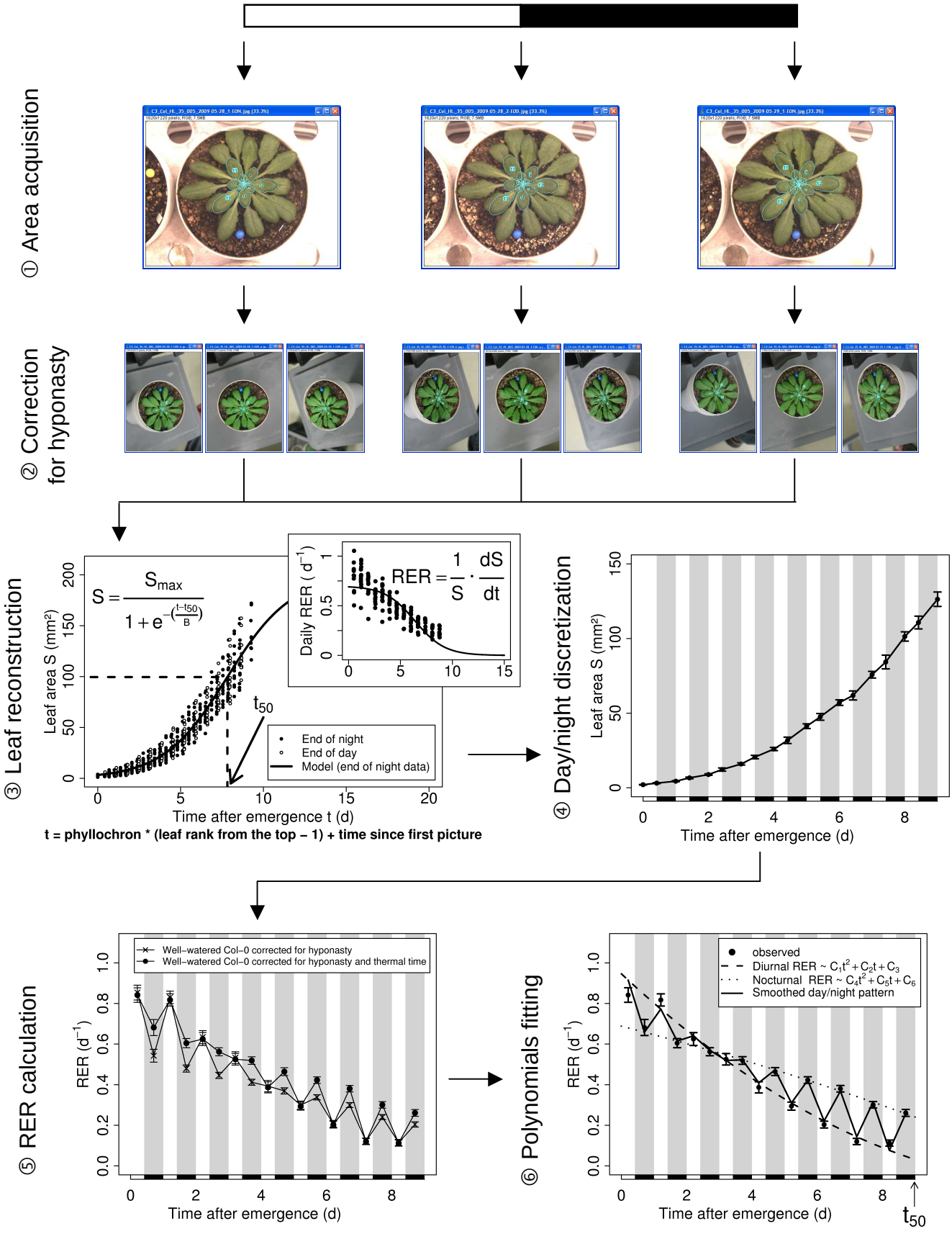
① Area acquisition
② Correction for hyponasty
③ Leaf reconstruction
④ Day/night discretization
⑤ RER calculation
⑥ Polynomials fitting
Leaf area S (mm²)
Time after emergence t (d)
Daily RER (d⁻¹)
End of night
End of day
Model (end of night data)
t50
t = phyllochron * (leaf rank from the top – 1) + time since first picture
Time after emergence (d)
RER (d⁻¹)
Well–watered Col–0 corrected for hyponasty
Well–watered Col–0 corrected for hyponasty and thermal time
observed
Diurnal RER ~ C1t²+C2t+C3
Nocturnal RER ~ C4t²+C5t+C6
Smoothed day/night pattern

Fig. S1. Process from plant images to RER patterns. When plants reached the targeted vegetative stage, three consecutive zenithal photographs were taken: the first at the beginning of a day period, the second at the end of the same day period, and the third at the end of the subsequent night. This was repeated three days later under maintained environmental regimes as a replicate, but for sake of clarity, only one session has been represented. ① **Area acquisition.** The area of serial leaves was extracted from the three pictures using a semi-automated program developed on the ImageJ software. ② **Correction for hyponasty.** An independent series of non-zenithal photographs was taken at the same three periods to measure leaf insertion angle and compute the actual leaf area. Step ② is fully described in Fig. S3 and was completed only on the wild-type Col-0 and on genotypes or environments that induced hyponasty. ③ **Leaf reconstruction.** For each picture and for each rank, leaf age after emergence was computed using the measured phyllochron. Leaf area was then plotted against its time after emergence, distinguishing end of day (open circles) from end of night (closed circles) values. the A logistical function (solid line) was fitted to the end of night dataset and the time of half expansion (t_{50}) was stored. Inset: daily relative expansion rate. RER was computed on a 24 h basis as the local slope of the natural logarithm of the area using the end of night dataset (closed circles). Analytical form of the RER (solid line) was derived from the previous logistical function and plotted using the same fitted parameters. Note that daily RER is continuously decreasing function of time. ④ **Day/night discretization.** Each area measured at the end of the day or night was assigned to the nearest reconstructed end of day or night, respectively. ⑤ **RER calculation.** RER was computed on a day/night basis using raw data (crosses) and corrected for the linear effects of temperature (thermal time, closed circles) using a threshold temperature of 3 °C and a reference temperature of 20 °C (see Methods). Values were affected to the middle of the light or dark period. ⑥ **Polynomials fitting.** A second-degree polynomial was fitted independently to the diurnal RER (dashed line) and to the nocturnal RER (dotted line). RER patterns were drawn from leaf emergence to t_{50} by joining the predicted values for the successive light and dark periods (solid line). For steps ④ to ⑥, black rectangles and gray bands indicate the night periods, and error bars are mean ± SE ($n \geq 10$).

Figure S2

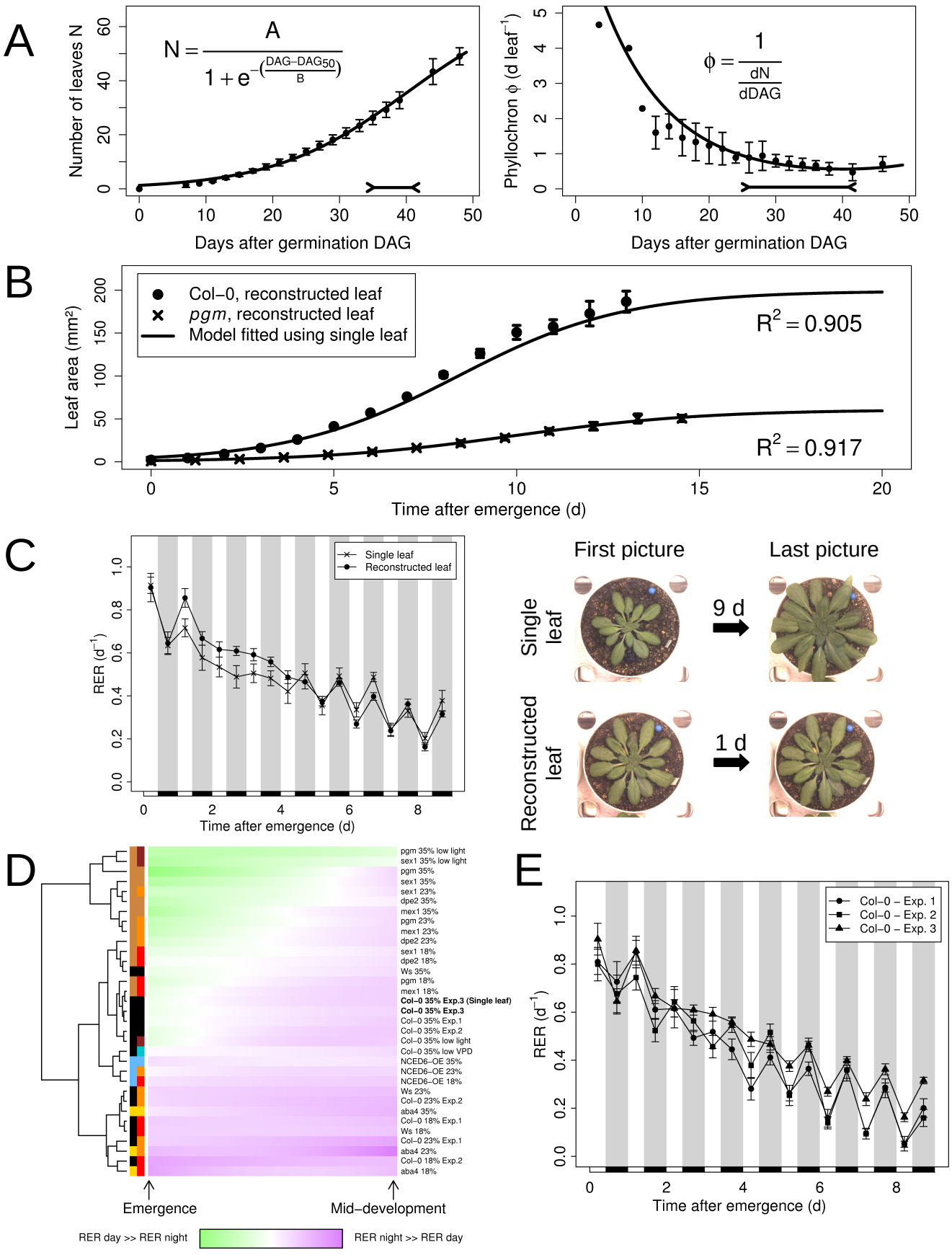
A
Number of leaves N
Days after germination DAG
Phyllochron ϕ (d leaf⁻¹)
Days after germination DAG
B
Col–0, reconstructed leaf
pgm, reconstructed leaf
Model fitted using single leaf
R² = 0.905
R² = 0.917
Leaf area (mm²)
Time after emergence (d)
C
Single leaf
Reconstructed leaf
RER (d⁻¹)
Time after emergence (d)
First picture
Last picture
Single leaf
9 d
Reconstructed leaf
1 d
D
Emergence
Mid–development
RER day >> RER night
RER night >> RER day
E
Col–0 – Exp. 1
Col–0 – Exp. 2
Col–0 – Exp. 3
RER (d⁻¹)
Time after emergence (d)

Fig. S2. Validation of the leaf reconstruction method. The relevance of the process of leaf temporal reconstruction from spatial information (Fig. S1) was verified at several levels. Error bars are mean ± SE ($n \geq 10$). **(A) Number of emerged leaves and phyllochron during rosette development.** Left panel: Emerged leaves were counted regularly until 50 days after germination (closed circles) on the well-watered Col-0. A logistical model was fitted to the data (solid line). The double-sense arrow indicates the period where the photographs were taken. Right panel: Phyllochron was computed as the inverse of leaf emergence rate, from data (closed circle) and model (solid line) of leaf number. The model was then inversed to compute the emergence date of the oldest digitalized leaf. The double-sense arrow shows the period from this oldest date until the day of measurement and underlines the phyllochron stability during this period. **(B) Area of a reconstructed leaf against a single leaf.** Leaf area was monitored either on one individual leaf during nine days (single leaf) or using serial leaves during one day (reconstructed leaf). Symbols show the area of the reconstructed leaf for Col-0 (closed circles) and *pgm* (crosses) under well-watered conditions. Solid lines show a logistical model fitted on the respective single leaf datasets. The indicated R^2 measures the quality of the model when the parameters obtained from the single leaf adjustment are applied to the reconstructed leaf dataset. **(C) Relative expansion rate of a reconstructed leaf against a single leaf.** The day/night RER in the well-watered Col-0 was compared between a reconstructed leaf and a single leaf as in (B). Black rectangles and gray bands indicate the night periods. Photographs show the whole rosette at the beginning and at the end of measurements for each method. Note that for the reconstructed leaf method, a second session was performed three days later as a replicate, leading to a four-day range between the first and the last picture, but it can be restricted to one day as depicted here. **(D) Heatmap of the expansion patterns including the single leaf dataset.** Same as Fig. 4A with addition of the single leaf data presented in (C). Note that both methods (text in bold on the right hand of the heatmap) clusterised closely together. **(E) Reproducibility of the leaf reconstruction method.** Day/night expansion patterns of a reconstructed leaf for three independent experiments performed on Col-0 under well-watered conditions. Black rectangles and gray bands indicate the night periods. Note that the three experiments clusterised closely together in the heatmap presented in (D).

Figure S3

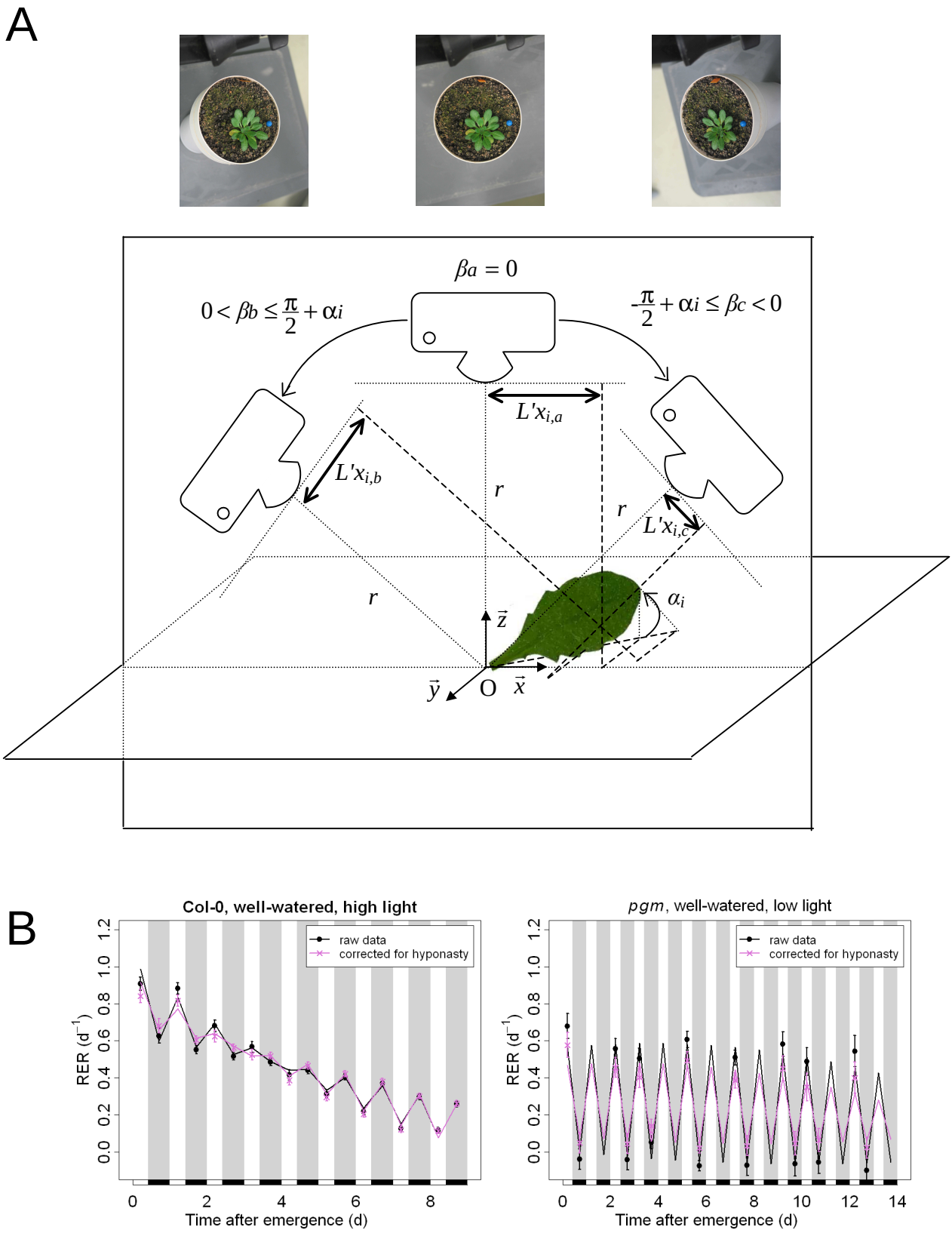
A
$\beta a = 0$
$0 < \beta b \leq \frac{\pi}{2} + \alpha i$
$-\frac{\pi}{2} + \alpha i \leq \beta c < 0$
$L'x_{i,a}$
$L'x_{i,b}$
$L'x_{i,c}$
r
r
r
α_i
$\vec{z}$
$\vec{y}$
O
$\vec{x}$
B
Col-0, well-watered, high light
pgm, well-watered, low light
raw data
corrected for hyponasty
RER (d^{-1})
Time after emergence (d)

Fig. S3. Taking hyponasty into account.

(A) Protocol to measure leaf insertion angle. Let us consider a reference frame $(\vec{x},\vec{y},\vec{z})$ of origin O related to the rosette center. Consider a digital camera whose diaphragm belongs to the circle of radius *r*, of center O and in the $(\vec{x},\vec{z})$ plane. Let β be the oriented angle between the $\vec{z}$ axis and the straight line defined by the origin and the camera diaphragm, so that for a zenithal picture, $\beta = 0$. Our camera was fixed in this way, using a rotating stand allowing to control β. Leaf length $L'x_i$ on the $\vec{x}$ component at the leaf rank *i* as measured on the photograph varies with β. Assuming that petiole and blade are aligned, the relation between the photographed leaf length $L'x_i$ and the actual leaf length Lx_i on the $\vec{x}$ component is given by:

$$\forall\ \beta \in \left[-\frac{\pi}{2}+\alpha i\ ;\ \frac{\pi}{2}+\alpha i\right]:\quad L'xi = Lxi \cdot \cos\left(\alpha i - \beta\right)$$

with α_i the insertion angle at the leaf rank *i*. One can check that the maximum of $L'x_i$ as a function of β equals Lx_i and is reached when the focal plane of the camera is parallel to the leaf plane (i.e. $\beta = \alpha_i$). Hence, using a set of three pictures { *a* ; *b* ; *c* } taken with an orientation of $\left\{\beta a = 0\ ;\ 0 < \beta b \le \frac{\pi}{2}+\alpha i\ ;\ -\frac{\pi}{2}+\alpha i \le \beta c < 0\right\}$, respectively, we were able to compute the insertion angle of each leaf rank *i* whose length on the $\vec{x}$ component was not zero, by solving numerically the following equation for α_i:

$$\frac{L'xi,b - L'xi,c}{L'xi,a} = \frac{\cos\left(\alpha i - \beta b\right) - \cos\left(\alpha i - \beta c\right)}{\cos\left(\alpha i\right)}$$

with $L'x_{i,a}$, $L'x_{i,b}$, and $L'x_{i,c}$ the length on the $\vec{x}$ component as measured on the pictures *a*, *b*, and *c*, respectively. From at least six replicates, an averaged value was computed for each leaf rank of a given genotype in a given environment, at the end of the day and at the end of the night. Then, the measured area from the zenithal pictures *S'i* of each leaf rank *i* under each condition investigated was corrected for α_i to obtain the actual area *Si* prior to the RER calculation using the simple trigonometric relationship:

$$Si = \frac{S'i}{\cos\left(\alpha i\right)}$$

(B) Examples showing the effects of leaf insertion angle on RER patterns. This protocol was applied to the well-watered Col-0 under high light as a control, and to the genotypes or treatments clearly inducing hyponasty (*pgm*, *sex1*, low light). As expected, the correction on the control had only minor effects (right panel) since Col-0 did not display a marked hyponasty. The effects were more pronounced on *pgm* under low light, a genotype × environment combination where hyponasty was enhanced, with a maximal difference of about 15 ° between night and day.

Figure S4

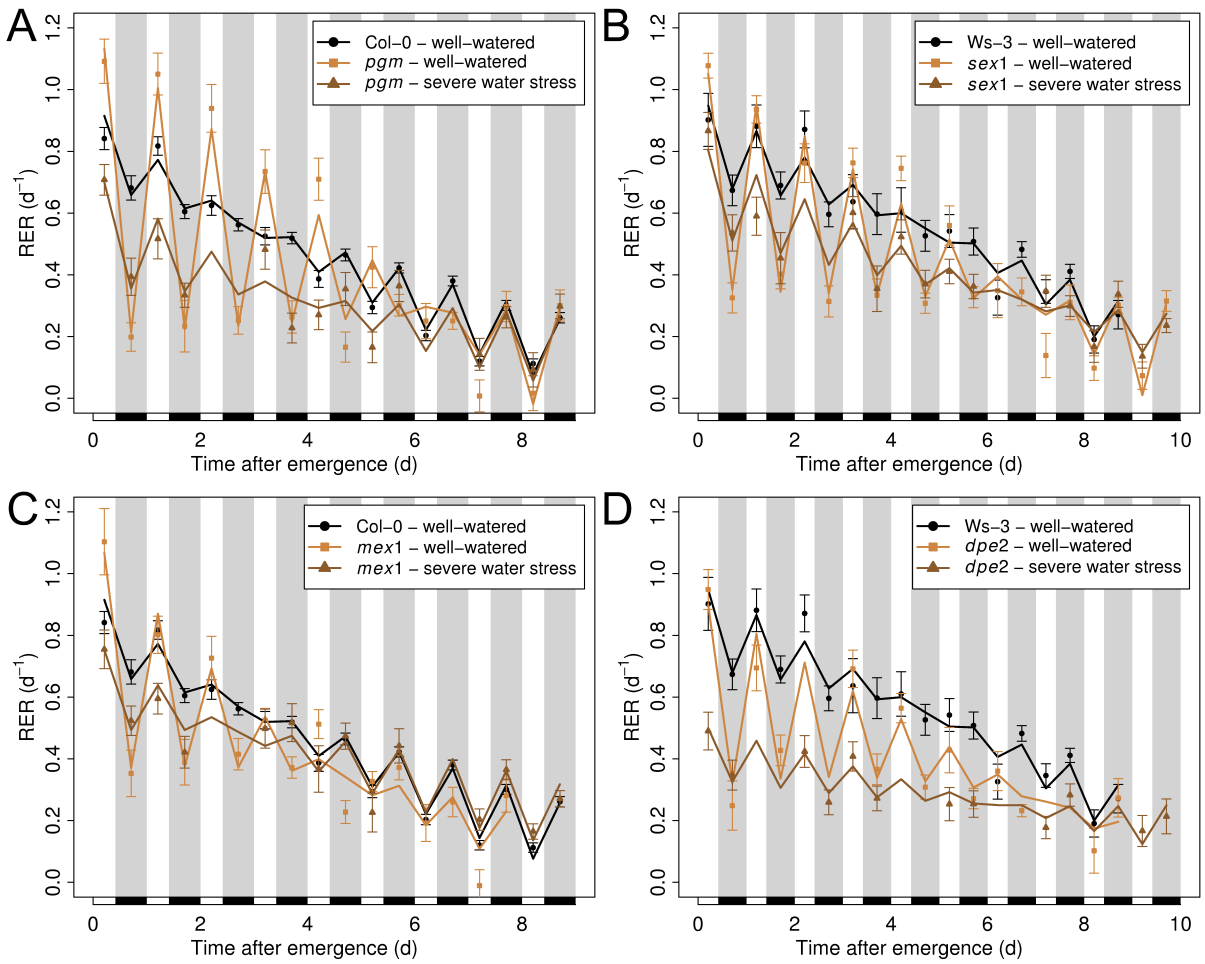

Fig. S4. Effect of a severe metabolic and hydraulic constraint in combination. The starch mutants were grown either under well-watered conditions (light tan) or under severe water stress (dark tan), and compared to their well-watered wild-type (black). Note the closeness between the starch mutants under soil water deficit and their well-watered wild-types. Black rectangles and gray bands indicate the night periods. Points: observed. Lines: smoothed. Error bars are mean ± SE (n ≥ 10). **(A) *pgm*. (B) *sex1*. (C) *mex1*. (D) *dpe2*.**

Figure S5

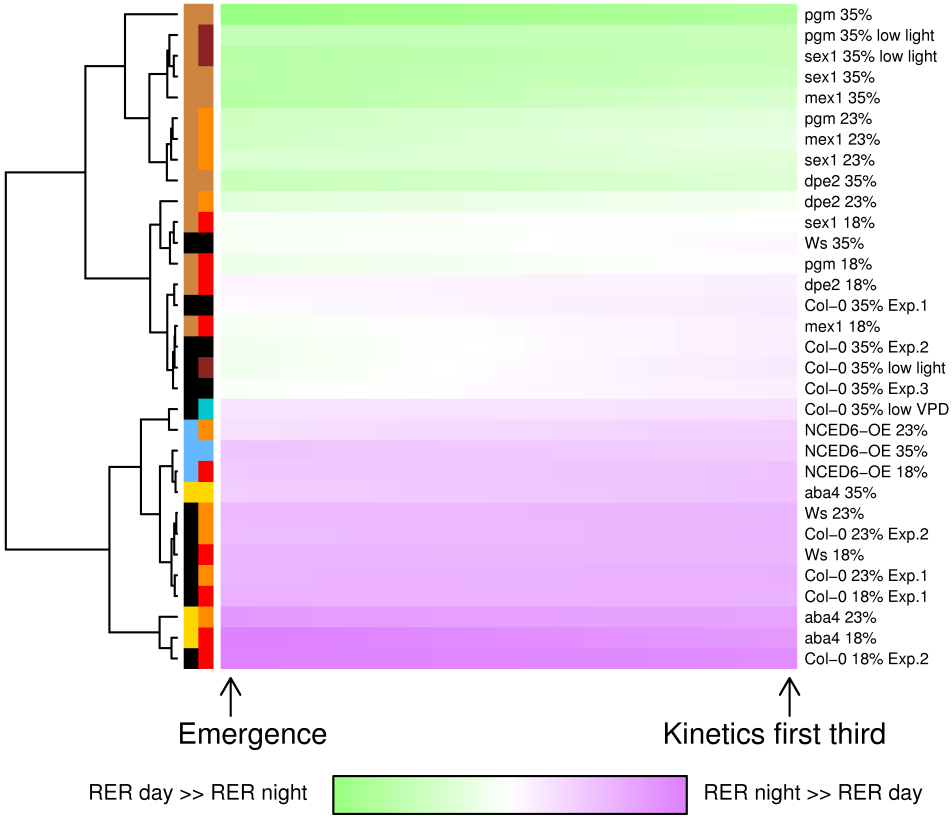

Fig. S5. Heatmap of the expansion patterns for the first third of the kinetics. Same as Fig. 4A but the analysis was restricted to the early stages. Note that in these conditions, well-watered wild-types clusterised foremost with the starch mutants instead of the wild-types under water stress.